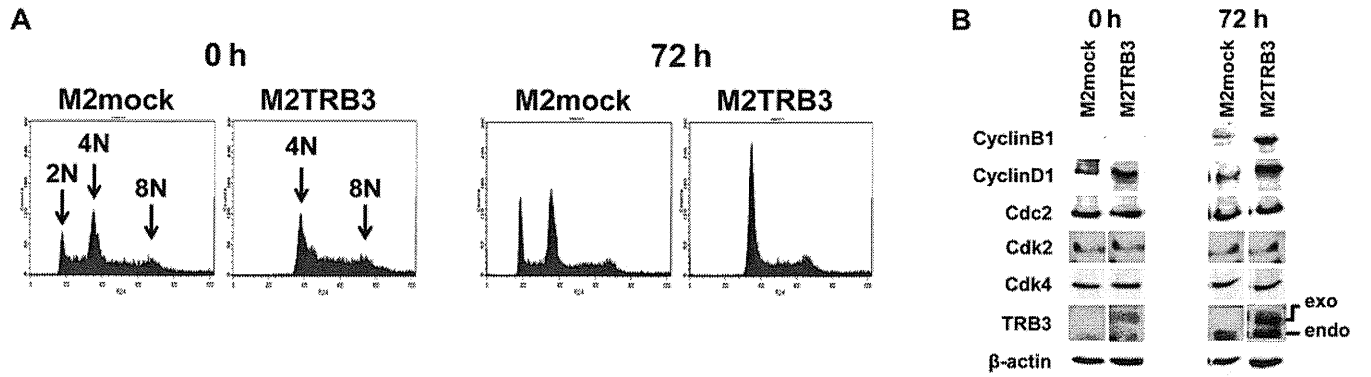

Figure 5. Effects of the TRB3 gene on DNA ploidy and protein expression. (A) Representative results of the flow cytometric analysis. After synchronizing cells in the G0/G1 phase, ploidy status was determined by flow cytometric analysis at 0 (left two panels) and 72 h (right two panels) in the M2mock and M2TRB3 cell lines. Note three peaks (2N, diploid; 4N, tetraploid; 8N, octaploid) in different locations in the DNA histogram. (B) Protein expression status of cell cycle control molecules and TRB3 in M2mock and M2TRB3 cell lines. Cell lysates were extracted at the indicated times (h) of the cell culture and then examined by western blot analysis for the indicated proteins, using the respective antibodies, as described in Materials and methods. β-actin was used as an internal control. Exogenous human TRB3 and endogenous mouse TRB3 are describes as exo and endo, respectively.

Table I. Distribution and rate (%) of ploidy in the M2TRB3 and M2mock cell lines.

		Time (h) after starvation	
Cell line	Ploidy	0 h	72 h
M2mock	2N	12.1±0.3[a]	16.6±0.1[b]
M2TRB3	2N	0.0±0.0	0.0±0.0
M2mock	4N	37.0±0.1	38.5±0.2[b]
M2TRB3	4N	41.6±2.5	57.5±0.5
M2mock	8N	6.0±0.1[a]	3.5±0.0[b]
M2TRB3	8N	25.3±1.8	16.2±0.3

Differences in the percentage of ploidy in M2TRB3 and M2mock cell lines. M2TRB3 vs. M2mock, [a]P<0.01 and [b]P<0.001.

labeling index as described in Materials and methods. The PCNA labeling index of the M2TRB3 tumors was higher than that of the M2 and M2mock tumors but this difference was not statistically significant (Fig. 3 lower panels and Fig. 4).

TRB3 affects the ploidy distribution of mouse mammary tumor cells. Due to the differences in tumor morphology noted in Fig. 3, we examined the effects of the TRB3 gene on DNA ploidy in M2mock and M2TRB3 cells. After synchronizing cells in the G0/G1 phase, we conducted experiments at 0 and 72 h using flow cytometric analysis. Representative DNA histograms of the analysis for these cells are shown in Fig. 5A, and distribution and rate of DNA ploidy are shown in Table I. In M2mock cells, the average percentage of diploid nuclei measured 12-16%. In contrast, no diploid nuclei were observed in M2TRB3 cells (Table I and Fig. 5A, far right panels). M2TRB3 cells showed a significant increase by 19 and 12% in the population of octaploid nuclei at 0 and 72 h, respectively, when compared to M2mock cells (Table I). There was also an increase (4-19%) in the population of tetraploid nuclei in the M2TRB3 cells. These results indicate that TRB3 affects the status of DNA ploidy in mouse mammary tumor cells. M2mock cells exhibited population peaks of aneuploid nuclei (2N, 4N and 8N), indicating that these cells harbor a variable number of chromosomes.

Expression status of TRB3 and cell cycle control molecules in M2TRB3 and M2mock cells. Due to the growth enhancing effects of TRB3 as noted in Fig. 2 and nuclear hyperploidy in M2TRB3 cells, we examined whether these cells affected the levels of expression of TRB3 and cell cycle control molecules. Thus, we measured the protein expression levels of TRB3 and cell cycle control molecules cyclin B1, cyclin D1, Cdc2, Cdk2 and Cdk4. In M2TRB3 cells, both exogenous and endogenous TRB3 were highly expressed at 72 h compared to M2mock cells that only expressed endogenous TRB3 (Fig. 5B, right two columns). In contrast, a weak expression level of endogenous TRB3 was observed at 0 h in the M2mock cells, and marginal expression was noted in both exogenous and endogenous TRB3 at the same time point in these cells. Cyclin B1 and cyclin D1 expression levels in the M2TRB3 cells increased at 72 h of the cell culture, in which tumor cells were out of synchrony, compared to those of the M2mock cells (Fig. 5B). Expression levels of Cdc2, Cdk2, and Cdk4 showed no change between the M2TRB3 and M2mock cells.

Discussion

Several human tumor tissues have recently been shown to highly express TRB3 mRNA (14). It has also been demonstrated by us that TRB3 regulates the stability of Cdc25A, an essential activator of CDKs (10). However, the precise role and functional morphology of TRB3 have not been established yet. Thus, we carried out the present study to provide further evidence concerning cell growth and morphological changes in mouse mammary tumor cells by focusing on the expression levels of TRB3 and cell cycle control molecules, cellular nucleus size, and the status of DNA ploidy. M2TRB3 cells showed a significant numerical increase compared to the control M2mock cells. As a result, the doubling time of the M2TRB3 and M2mock cell lines was approximately 12

and 15 h, respectively (Fig. 2A). A similar condition was also observed in the tumors, clearly indicating that in this context TRB3 had an enhancing property on the growth of mouse mammary tumor cells.

It is well understood that cell volume increases with DNA ploidy, and this correlation has been observed in a wide variety of eukaryotic cells (19). Increased DNA ploidy can exert its effects by increasing nuclear size, chromatin content, and the expression levels of a certain gene (19). We found that in the M2TRB3 tumors the mean diameter of the nucleus measured 9.4±0.3 μm and that of the M2mock tumors was 7.0±0.2 μm. From the flow cytometric analysis we also found a significant increase in the population of M2TRB3 cells bearing tetraploid or octaploid nuclei compared to that of the M2mock cells bearing mostly diploid or tetraploid nuclei (Fig. 5A). These findings are consistent with those reported by Danielsen *et al* (20) who demonstrated that nuclei of 6.0-7.5 μm in diameter are classified as diploid, 7.5-9.0 μm as tetraploid, and 9.5-11.0 μm as octaploid. Collectively, TRB3 may have the ability of polyploidization during development.

Cyclins are the key molecules in cell cycle control due to their specific and periodic expression during cell cycle progression. Cyclin D1 complexes with Cdk4 and Cdk6 and thereby regulates transition from the G1 phase into the S phase by phosphorylation and inactivation of pRB (21-24). Phosphorylation causes release of the transcription factor E2F that promotes mitosis (24,25). Gene amplification and/or protein overexpression of cyclin D1 occurs in a variety of human carcinomas and tumors in animal models (26,27). Unlike cyclin D1, the activity of cyclin B1 is essential for G2/M phase of the cell cycle through a complex with Cdc2 (28). However, little is known about the association between DNA ploidy and cyclin B1/cyclin D1 expression status. We found elevated expression levels of cyclin B1 and cyclin D1 in M2TRB3 cells without significant changes in expression levels of Cdc2, Cdk2 and Cdk4 (Fig. 5B). Furthermore, M2TRB3 cells totally lack diploid nuclei but a population of the M2mock cells consisted mainly of diploid or tetraploid nuclei, suggesting that expression of cyclin B1 and cyclin D1 may positively correlate with the generation of hyperploid nuclei and thereby further promote the chromosomal instability in TRB3-overexpressing cells. Similar results regarding cyclin B1/D1 overexpression and promotion of tetraploidy or aneuploidy (>2N) were previously obtained in human breast carcinoma and mouse myeloid cells (28,29). As we found in the present study, the novel aspect of the TRB3 gene is that this gene induces an increase in cell proliferation and polyploidy leading to enlargement of the nuclear size of the implanted mouse mammary tumor cells. These effects of TRB3 may cause chromosomal instability. The detailed mechanism of this chromosomal instability is not known but may be related to the above-described effects of TRB3 on morphological function. In a recent study, we demonstrated that TRB3 may regulate the activity of anaphase-promoting complex/cyclosome (APC/C^{Cdh1}) that is a major ubiquitin ligase complex regulating the progression of the cell cycle through the ubiquitination and subsequent degradation of cell cycle control molecules including cyclin B1 (30,31). In the present study, we found an elevated expression level of the cyclin B1 protein in M2TRB3 cells that overexpressed the human TRB3 gene. We should emphasize that two cell lines M2TRB3 and M2mock differ in synchrony status that may influence their response to morphological function. This intriguing respect may also reflect the role of cell cycle progression of TRB3. Thus, it is of interest to examine whether the TRB3 gene causes *de novo* morphological changes leading to tumorigenesis in a specific organ site. An additional study using the TRB3 transgenic animal model is currently in progress to answer this question.

Acknowledgements

We thank Dr Hiroyuki Tsuda for the valuable comments and discussions. We also acknowledge the excellent technical assistance of Kenta Moriwaki and Shuhei Ikenaga. This study was supported by a Grant-in-Aid from the Ministry of Education, Culture, Sports, Science, and Technology, and the Ministry of Health, Labour, and Welfare of Japan.

References

1. Grosshans J and Wieschaus E: A genetic link between morphogenesis and cell division during formation of the ventral furrow in *Drosophila*. Cell 101: 523-531, 2000.
2. Mata J, Curado S, Ephrussi A and Rørth P: Tribbles coordinates mitosis and morphogenesis in *Drosophila* by regulating string/CDC25 proteolysis. Cell 101: 511-522, 2000.
3. Seher TC and Leptin M: Tribbles, a cell-cycle brake that coordinates proliferation and morphogenesis during *Drosophila* gastrulation. Curr Biol 10: 623-629, 2000.
4. Bowers AJ, Scully S and Boylan JF: SKIP3, a novel *Drosophila* tribbles ortholog, is overexpressed in human tumors and is regulated by hypoxia. Oncogene 22: 2823-2835, 2003.
5. Bezy O, Vernochet C, Gesta S, Farmer SR and Kahn CR: TRB3 blocks adipocyte differentiation through the inhibition of C/EBPβ transcriptional activity. Mol Cell Biol 27: 6818-6831, 2007.
6. Chan MC, Nguyen PH, Davis BN, Ohoka N, Hayashi H, Du K, Lagna G and Hata A: A novel regulatory mechanism of the bone morphogenetic protein (BMP) signaling pathway involving the carboxyl-terminal tail domain of BMP type II receptor. Mol Cell Biol 27: 5776-5789, 2007.
7. Du K, Herzig S, Kulkarni RN and Montminy M: TRB3: a tribbles homolog that inhibits Akt/PKB activation by insulin in liver. Science 300: 1574-1577, 2003.
8. Qi L, Heredia JE, Altarejos JY, Screaton R, Goebel N, Niessen S, Macleod IX, Liew CW, Kulkarni RN, Bain J, Newgard C, Nelson M, Evans RM, Yates J and Montminy M: TRB3 links the E3 ubiquitin ligase COP1 to lipid metabolism. Science 312: 1763-1766, 2006.
9. Tang M, Zhong M, Shang Y, Lin H, Deng J, Jiang H, Lu H, Zhang Y and Zhang W: Differential regulation of collagen types I and III expression in cardiac fibroblasts by AGEs through TRB3/MAPK signaling pathway. Cell Mol Life Sci 65: 2924-2932, 2008.
10. Ohoka N, Yoshii S, Hattori T, Onozaki K and Hayashi H: TRB3, a novel ER stress-inducible gene, is induced via ATF4-CHOP pathway and is involved in cell death. EMBO J 24: 1243-1255, 2005.
11. Sakai S, Ohoka N, Onozaki K, Kitagawa M, Nakanishi M and Hayashi H: Dual mode of regulation of cell division cycle 25 A protein by TRB3. Biol Pharm Bull 33: 1112-1116, 2010.
12. Jin G, Yamazaki Y, Takuwa M, Takahara T, Kaneko K, Kuwata T, Miyata S and Nakamura T: Trib1 and Evi1 cooperate with Hoxa and Meis1 in myeloid leukemogenesis. Blood 109: 3998-4005, 2007.
13. Keeshan K, He Y, Wouters BJ, Shestova O, Xu L, Sai H, Rodriguez CG, Maillard I, Tobias JW, Valk P, Carroll M, Aster JC, Delwel R and Pear WS: Tribbles homolog 2 inactivates C/EBPα and causes acute myelogenous leukemia. Cancer Cell 10: 401-411, 2006.
14. Xu J, Lv S, Qin Y, Shu F, Xu Y, Chen J, Xu BE, Sun X and Wu J: TRB3 interacts with CtIP and is overexpressed in certain cancers. Biochim Biophys Acta 1770: 273-278, 2007.

15. Suzui M, Sunagawa N, Chiba I, Moriwaki H and Yoshimi N: Acyclic retinoid, a novel synthetic retinoid, induces growth inhibition, apoptosis, and changes in mRNA expression of cell cycle- and differentiation-related molecules in human colon carcinoma cells. Int J Oncol 28: 1193-1199, 2006.
16. Suzui M, Inamine M, Kaneshiro T, Morioka T, Yoshimi N, Suzuki R, Kohno H and Tanaka T: Indole-3-carbinol inhibits the growth of human colon carcinoma cells but enhances the tumor multiplicity and volume of azoxymethane-induced rat colon carcinogenesis. Int J Oncol 27: 1391-1399, 2005.
17. Suzui M, Masuda M, Lim JT, Albanese C, Pestell RG and Weinstein IB: Growth inhibition of human hepatoma cells by acyclic retinoid is associated with induction of p21(CIP1) and inhibition of expression of cyclin D1. Cancer Res 62: 3997-4006, 2002.
18. Futakuchi M, Nannuru KC, Varney ML, Sadanandam A, Nakao K, Asai K, Shirai T, Sato SY and Singh RK: Transforming growth factor-beta signaling at the tumor-bone interface promotes mammary tumor growth and osteoclast activation. Cancer Sci 100: 71-81, 2009.
19. Jorgensen P and Tyers M: How cells coordinate growth and division. Curr Biol 14: 1014-1027, 2004.
20. Danielsen H, Lindmo T and Reith A: A method for determining ploidy distributions in liver tissue by stereological analysis of nuclear size calibrated by flow cytometric DNA analysis. Cytometry 7: 475-480, 1986.
21. Hunter T and Pines J: Cyclins and cancer. II: cyclin D and CDK inhibitors come of age. Cell 79: 573-582, 1994.
22. Weinberg RA: The retinoblastoma protein and cell cycle control. Cell 81: 323-330, 1995.
23. Chellappan SP, Hiebert S, Mudryj M, Horowitz JM and Nevins JR: The E2F transcription factor is a cellular target for the RB protein. Cell 65: 1053-1061, 1991.
24. Wilson CS, Butch AW, Lai R, Medeiros LJ, Sawyer JR, Barlogie B, McCourty A, Kelly K and Brynes RK: Cyclin D1 and E2F-1 immunoreactivity in bone marrow biopsy specimens of multiple myeloma: relationship to proliferative activity, cytogenetic abnormalities and DNA ploidy. Br J Haematol 112: 776-782, 2001
25. Johnson DG, Schwarz JK, Cress WD and Nevins JR: Expression of transcription factor E2F1 induces quiescent cells to enter S phase. Nature 365: 349-352, 1993.
26. Staibano S, Lo Muzio L, Pannone G, Mezza E, Argenziano G, Vetrani A, Lucariello A, Franco R, Errico ME and De Rosa G: DNA ploidy and cyclin D1 expression in basal cell carcinoma of the head and neck. Am J Clin Pathol 115: 805-813, 2001.
27. Bartkova J, Lukas J, Strauss M and Bartek J: Cyclin D1 oncoprotein aberrantly accumulates in malignancies of diverse histogenesis. Oncogene 10: 775-778, 1995.
28. Collecchi P, Santoni T, Gnesi E, Giuseppe Naccarato A, Passoni A, Rocchetta M, Danesi R and Bevilacqua G: Cyclins of phases G1, S and G2/M are overexpressed in aneuploid mammary carcinomas. Cytometry 42: 254-260, 2000.
29. Yin XY, Grove L, Datta NS, Katula K, Long MW and Prochownik EV: Inverse regulation of cyclin B1 by c-Myc and p53 and induction of tetraploidy by cyclin B1 overexpression. Cancer Res 61: 6487-6493, 2001.
30. Ohoka N, Sakai S, Onozaki K, Nakanishi M and Hayashi H: Anaphase-promoting complex/cyclosome-cdh1 mediates the ubiquitination and degradation of TRB3. Biochem Biophys Res Commun 392: 289-294, 2010.
31. Lukas C, Sørensen CS, Kramer E, Santoni-Rugiu E, Lindeneg C, Peters JM, Bartek J and Lukas J: Accumulation of cyclin B1 requires E2F and cyclin-A-dependent rearrangement of the anaphase-promoting complex. Nature 401: 815-818, 1999.

genesis 51:268–274 (2013)

TECHNOLOGY REPORT

A Novel Reporter Rat Strain That Expresses LacZ Upon Cre-Mediated Recombination

Katsumi Fukamachi,[1] Hajime Tanaka,[2] Yuto Sakai,[1,3] David B. Alexander,[4] Mitsuru Futakuchi,[1] Hiroyuki Tsuda,[4]* and Masumi Suzui[1]

[1]Department of Molecular Toxicology, Nagoya City University Graduate School of Medical Sciences, 1 Kawasumi, Mizuho-cho, Mizuho-ku, Nagoya 467-8601, Japan

[2]Department of Gastroenterology and Metabolism, Nagoya City University Graduate School of Medical Sciences, 1 Kawasumi, Mizuho-cho, Mizuho-ku, Nagoya 467-8601, Japan

[3]Department of Drug Metabolism and Disposition, Graduate School of Pharmaceutical Sciences, Nagoya City University, 3-1 Tanabe-dori, Mizuho-ku, Nagoya 467-8603, Japan

[4]Nanotoxicology Project, Nagoya City University, 3-1 Tanabe-dori, Mizuho-ku, Nagoya 467–8603, Japan

Received 26 July 2012; Revised 26 November 2012; Accepted 14 January 2013

Summary: The recent widespread application of Cre/*loxP* technology has resulted in a new generation of conditional animal models that can better recapitulate many salient features of human disease. These models benefit from the ability to monitor the expression and functionality of Cre protein. We have generated a conditional (Cre/*loxP* dependent) *LacZ* reporter rat (termed the LacZ541 rat) to monitor Cre in transgenic rats. When LacZ541 rats were bred with another transgenic rat line expressing Cre recombinase under the control of the CAG promoter, LacZ/Cre double transgenic embryos displayed ubiquitous expression of LacZ, and when LacZ541 rats were bred with transgenic rats expressing Cre/*loxP*-dependent oncogenic H- or K-*ras*, LacZ was expressed in the lesions resulting from the activation of the oncogene. The LacZ541 rat enables evaluation of the performance of Cre-expressing systems which are based upon transgenic rats or somatic gene transfer vectors and provides efficient and simple lineage marking. genesis 51:268–274. © 2013 Wiley Periodicals, Inc.

Key words: rat; transgenic; reporter; β-galactosidase; Cre; loxP

The rat is an important murine model for studies in oncology, physiology, pathobiology, toxicology, neurobiology, and a variety of other disciplines (Jacob and Kwitek, 2002). The rat is of value in these fields because it is larger than the mouse and because a plethora of organ-specific physiologic and disease models have been developed for it over the last century. Surgical procedures can be performed more easily than in mice and disease models sometimes more closely reflect the situation encountered in humans. The importance of the rat as a biological model has led to an intense effort to also establish it as a strong genetic model.

Genetically engineered animals are invaluable in assessing the role of genes in complex processes such as tumorigenesis and embryonic development. The recent widespread application of Cre/*loxP* technology (Rajewsky *et al.*, 1996) has resulted in a new generation of conditional animal preclinical models that can better recapitulate many salient features of human disease. Cre expression achieved by classic transgenesis or targeting to an appropriate locus can be tissue specific, temporally restricted or inducible (Feil *et al.*, 1996). For example, we have established a transgenic rat carrying

Additional Supporting Information may be found in the online version of this article.

*Correspondence to: Hiroyuki Tsuda, Nanotoxicology Project, Nagoya City University, 3-1 Tanabe-dori, Mizuho-ku, Nagoya 467-8603, Japan. E-mail: htsuda@phar.nagoya-cu.ac.jp

Contract grant sponsors: Japan Society for the Promotion of Science; the Ministry of Health, Labor and Welfare, Japan; the Ministry of Education, Culture, Sports, Science and Technology of Japan

Published online 24 January 2013 in Wiley Online Library (wileyonlinelibrary.com).

DOI: 10.1002/dvg.22371

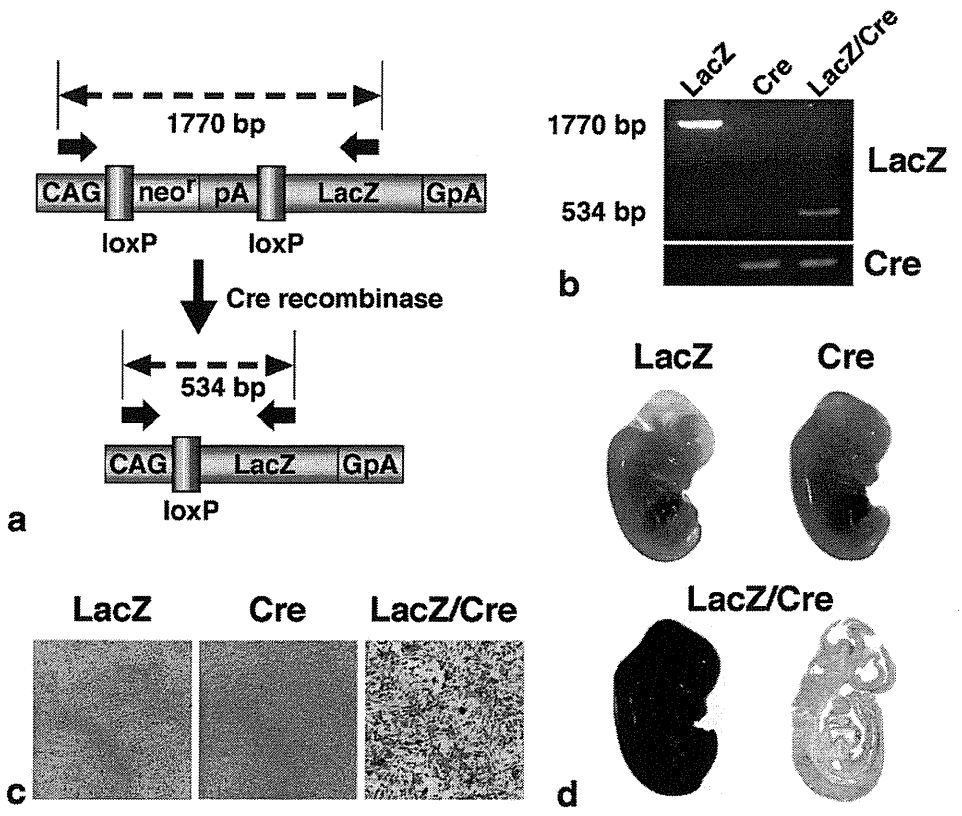

FIG. 1. Cre-mediated activation of the lacZ gene in rats. (**a**) The transgene is comprised of a CAG promoter, a cassette for the neomycin resistance gene flanked by loxP sites, and a sequence containing the LacZ open reading frame. Cre recombinase activity results in Cre-mediated recombination of the transgene and removal of the neo-coding region and its associated mRNA polyadenylation signal, generating a functional LacZ expression unit. pA, SV40 early poly(A) site; GpA, rabbit-β-globin poly(A) site. Arrows indicate primers for the detection of recombination of the transgene. (**b**) Mating a heterozygous male LacZ541 transgenic rat with a homozygous female Cre-expressing transgenic rat resulted in progeny in which recombination of the LacZ transgene had occurred. The LacZ541 transgenic embryo was used as the negative control. PCR analysis showed that a 534-bp band is present in the LacZ/Cre double transgenic embryo, but not in the LacZ or Cre transgenic embryos. The neomycin cassette of the LacZ transgene in the LacZ/Cre embryo was removed by Cre recombinase. (**c**) X-Gal staining of fibroblast cells derived from LacZ (left), Cre (middle) and LacZ/Cre (right) heterozygous embryos. (**d**) Whole mount X-Gal staining of E14 LacZ (left), Cre (right) and LacZ/Cre (bottom) heterozygous littermate embryos. A sagittal section of the LacZ/Cre embryo is also shown.

a human $H\textit{ras}^{G12V}$ or $K\textit{ras}^{G12V}$ oncogene regulated by the Cre/*loxP* system (Hras250 and Kras301 rats) (Tanaka *et al.*, 2010; Ueda *et al.*, 2006) in which pancreatic carcinogenesis is initiated by targeted activation of the transgene by injecting Cre-carrying adenovirus into the pancreatic ducts and acini through the common bile duct. This rat model provides a powerful research tool for examining the cytogenesis of pancreatic ductal adenocarcinoma.

In Cre/*loxP*-based experimental systems, it is important to monitor Cre activity at the desired time points and to verify the presence or absence of Cre activity during development. Such systems have been developed for the mouse: investigators have generated transgenic mouse lines in which β-galactosidase (lacZ) expression is conditional on Cre-dependent removal of an intervening segment (Akagi *et al.*, 1997; Araki *et al.*, 1995; Soriano, 1999; Tsien *et al.*, 1996), allowing Cre activity to be linked to lacZ activity. In the rat, a reporter line based on a DsRed/GFP double-reporter transgene under the control of the Cre/*loxP* system has also been established (Sato *et al.*, 2004). In this report we describe another reporter line, the LacZ541 rat, which carries a lacZ gene regulated by the Cre/*loxP* system. The advantage of LacZ is ease of visualization *in situ* and in section and whole mount preparations. The LacZ541 rat enables evaluation of the performance of Cre-expressing systems and provides efficient and simple lineage marking.

Reporter rats were generated by incorporating a transgene in which the CAG promoter is separated from a *lacZ* open reading frame by a stuffer sequence (neomycin resistant gene) flanked by *loxP* sites (Fig. 1A) which stops transcription of *lacZ*. A line was established (SD-Tg(CAG-lacZ)541Htsu, LacZ541) in which the transgene was transmittable to descendant

generations. In these rats, *Cre*-mediated recombination removes the stop sequence, generating a functional LacZ expression unit and allowing expression of β-galactosidase in all cell types in which the CAG promoter is active. Heterozygous male LacZ541 transgenic rats were bred with homozygous female NCre rats (Sato *et al.*, 2004): The NCre rat was made by incorporating a transgene in which the CAG promoter directly controls expression of Cre, and consequently, NCre rats express Cre ubiquitously. When the NCre rat was bred to the DsRed/GFP reporter rat, Cre deleted the DsRed sequence in the progeny resulting in ubiquitous expression of GFP (Sato *et al.*, 2004). Results of crossing the deleter NCre rat line with heterozygous LacZ541 rats are shown in Figure 1. Genomic DNA was isolated from the embryonic yolk sac and subjected to PCR. In LacZ541 embryos, a 1770-bp band corresponding to the unmodified transgene was detected, while in LacZ/Cre compound embryos, PCR generated a 534-bp band corresponding to the recombinant transgene (Fig. 1b); Cre embryos do not have the LacZ transgene. Embryos were also collected at embryonic day 14 and stained with X-Gal for LacZ activity. Rat embryonic fibroblast cells and embryos heterozygous for both LacZ and Cre alleles displayed ubiquitous staining, whereas wild-type (data not shown), heterozygous LacZ and Cre embryos did not show any staining (Fig. 1c,d). These results demonstrate that in LacZ541 transgenic rats, Cre induces recombination of the transgene resulting in CAG promoter driven expression of the *lacZ* gene. The LacZ541 rats did not display an overt phenotype and were bred to obtain viable and fertile homozygous transgenic progeny. The LacZ541 transgenic rat is available from the National BioResource Project for the Rat in Japan (NBRP Rat No: 0569) (http://www.anim.med.kyoto-u.ac.jp/NBR/).

To examine the expression of LacZ in adult organs, LacZ/Cre double transgenic (LacZ/Cre) rats were generated by breeding heterozygous LacZ541 rats with homozygous female NCre rats. Major organs were removed from LacZ/Cre, LacZ, and Cre rats and the LacZ expression pattern and intensity was determined by X-Gal staining (Figs. 2 and 3, and Supporting Information Fig. S1). Skeletal muscle and myocardium exhibited strong LacZ expression in LacZ/Cre rats. The expression pattern and intensity of LacZ is summarized in Table 1. The expression pattern of LacZ in LacZ/Cre rats was almost the same as the expression pattern of LacZ in CAG/LacZ-DA rats: in CAG/LacZ-DA rats, the expression of LacZ is directly driven by the CAG promoter (Inoue *et al.*, 2005). The LacZ/Cre rat embryo clearly showed widespread lacZ expression. However, some adult organs, including the liver, were negative. Because CAG promoter can be activated in stem cells including fertilized eggs, Cre is expected to remove the stop sequence in the CAG-neo-LacZ transgene and allow *lacZ* transcription to occur ubiquitously in the early embryo, and PCR analysis confirmed that recombination had occurred in all of the organs listed in Table 1 (Supporting Information Fig. S2). This indicates that the recombination frequency in these tissues was not related with LacZ expression and activity. Lack of LacZ expression, for example in the liver, could be because the site of transgene integration is not permissive for expression in the adult liver, or CAG promoter activity might be low in the adult liver of LacZ541 rats.

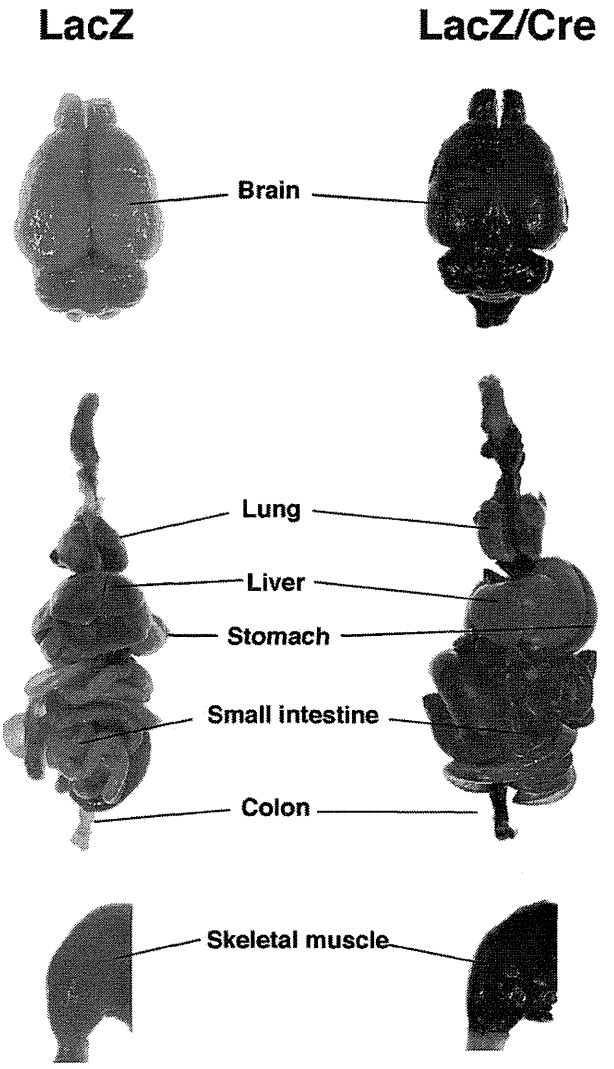

FIG. 2. Cre-mediated recombination in the adult organs. Whole mount X-Gal staining of the adult organs of LacZ and LacZ/Cre double transgenic rats. Tissues were stained overnight (brain) or for 3 h (other organs). Note that the olfactory bulb and cerebellum of the LacZ rat brain is light green because of endogenous β-galactosidase activity; the olfactory bulb and cerebellum of the LacZ rat brain did not stain blue/green when staining was limited to 3 h (not shown).

To examine whether the LacZ541 rat is useful for carcinogenesis studies, we used the LacZ541 rat to

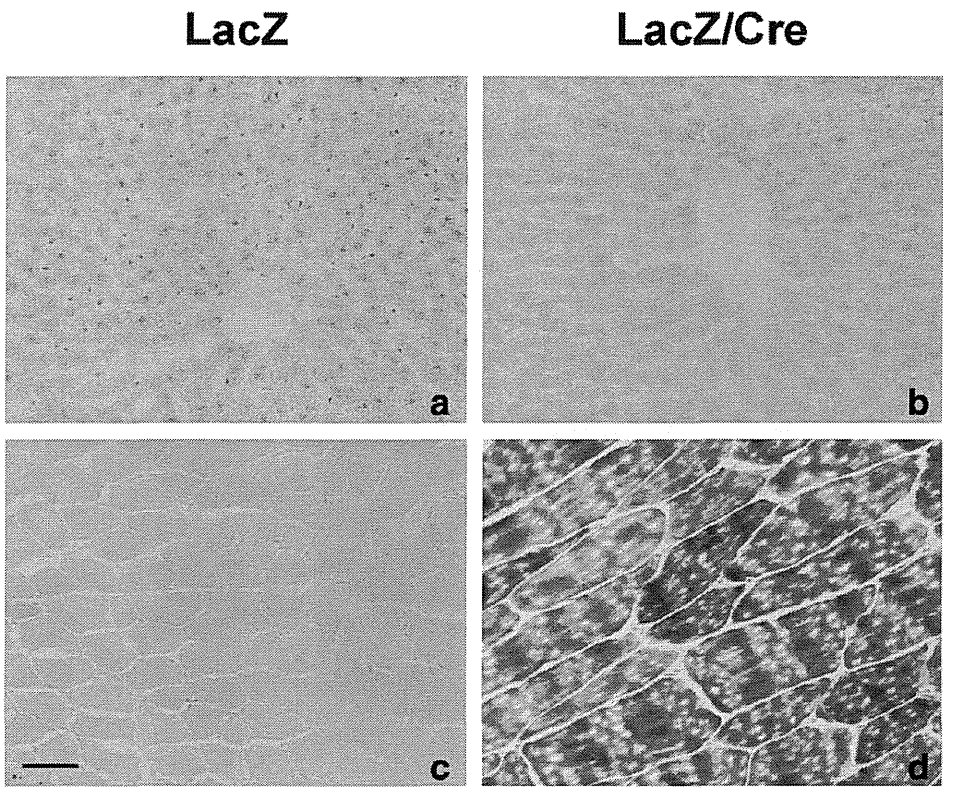

FIG. 3. LacZ expression in the adult tissues of LacZ and LacZ/Cre rats. Frozen sections were stained with X-gal. (**a**) and (**b**), Liver; (**c**) and (**d**), Skeletal muscle. Bar = 50 μm.

investigate the expression of the oncogenic H*ras*^{G12V} transgene in a rat model of pancreatic cancer. Our rat models of pancreatic cancer use three different Cre regulated human *ras*^{G12V} transgenes to induce cancer, H*ras*^{G12V}, K*ras*^{G12V}, and HA-tagged K*ras*^{G12V} (Fukamachi *et al.*, 2009; Tanaka *et al.*, 2010; Ueda *et al.*, 2006), with specific targeting of pancreatic cancer being achieved by injecting a recombinant adenovirus vector carrying Cre recombinase (AxCANCre) into the pancreatic duct via the common bile. Cells infected with AxCANCre express the oncogenic *ras*^{G12V} transgene when Cre removes the stop sequence which lies between the CAG promoter and the *ras*^{G12V} open reading frame. In the experiment described below, we used the H*ras*^{G12V} (Hras250) and HA-K*ras*^{G12V} (Kras301) rats.

In the HA-K*ras*^{G12V} rat, expression of the oncogenic transgene can be investigated by techniques, such as immunohistochemistry, which target the HA tag (Fukamachi *et al.*, 2009; Tanaka *et al.*, 2010). In the H*ras*^{G12V} rat, on the other hand, there are only two amino acid differences between the sequences of endogenous *ras* and the transgene; therefore, immunohistochemistry cannot be used to investigate the expression of the oncogenic transgene in this rat. We generated HA-Kras^{G12V}/LacZ and Hras^{G12V}/LacZ double transgenic rats (Kras/LacZ and Hras/LacZ rats) by breeding LacZ541 rats with Kras301 or Hras250 rats. Kras/LacZ and Hras/LacZ rats were injected with AxCANCre, and 3 weeks after injection, the animals were killed. Multiple grossly visible whitish nodules were observed throughout the pancreas in all of the Kras/LacZ and Hras/LacZ rats. Histological examination showed that

Table 1
Pattern of LacZ Expression in Organs From LacZ/Cre-Tg Rats

Organ	LacZ expression
Brain	+
Myocardium	+++
Skeletal muscle	+++
Blood vessels	−
Lung	+
Liver	−
Spleen	−
Pancreas	±
Kidney	++
Adrenal grand	+
Stomach	+
Small intestine	+
Colon	+++
Ovary	+
Uterus	+

−, negative; ±, weakly positive; + mildly positive; ++, moderately positive; +++, strongly positive.

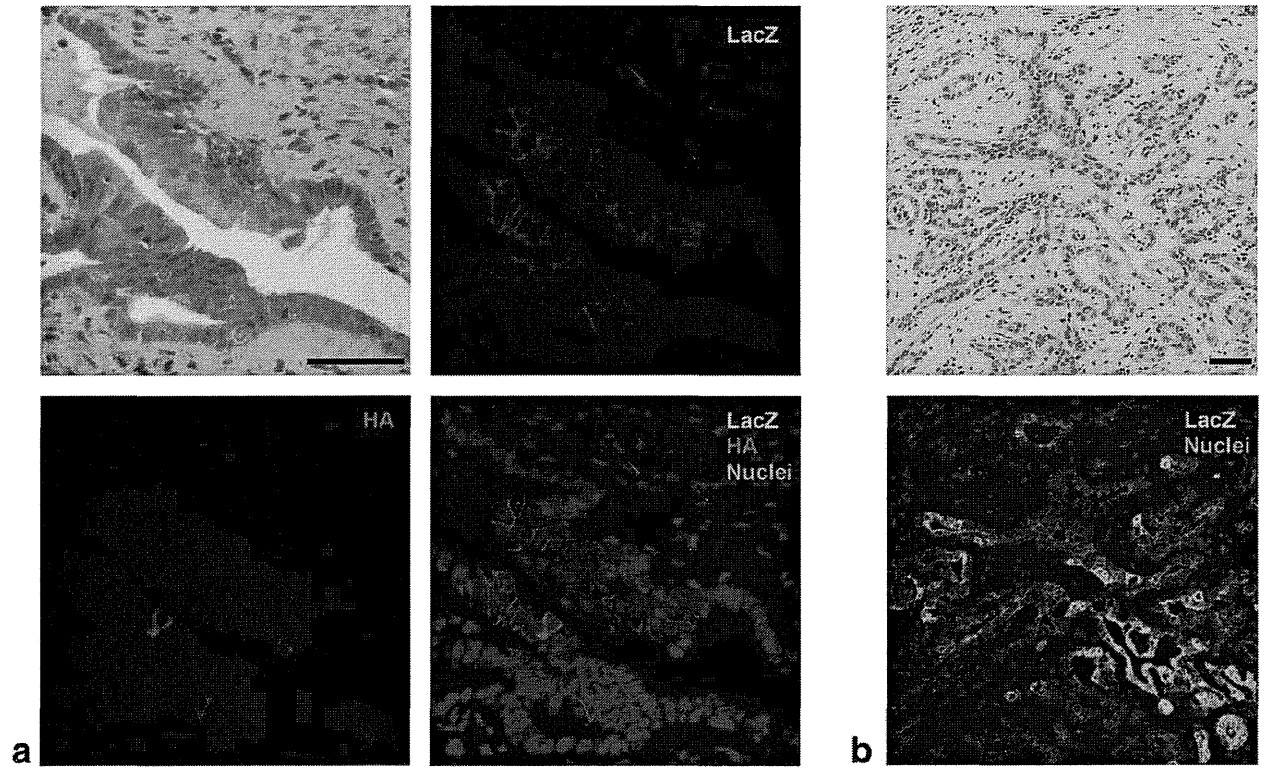

FIG. 4. Analysis of LacZ expression in pancreas ductal adenocarcinoma of ras/LacZ double transgenic rats. (**a**) Colocalization of LacZ (green) and HA-K*ras*^{G12V} (red) in pancreatic lesions of the Kras/LacZ rat. (**b**) Immunofluorescence staining of β-galactosidase in the pancreas shows LacZ positive cells (green) clustered in ductal lesions of the Hras/LacZ rat. Bar = 50 μm.

these nodules were adenocarcinomas, as in our previous reports (Tanaka *et al.*, 2010; Ueda *et al.*, 2006). In Kras/LacZ rats, double immunofluorescence staining for LacZ and HA showed that the expression pattern of LacZ closely resembled that of HA-K*ras*^{G12V} (Fig. 4a), demonstrating that in HA-K*ras*^{G12V}/LacZ double transgenic rats, the expression of the LacZ and HA-K*ras*^{G12V} transgenes is linked; in cells which are infected by AxCANCre and express Cre, Cre generally activates both the HA-K*ras*^{G12V} transgene and the LacZ transgene. Thus, LacZ can be used to monitor the expression of Cre/*loxP*-dependent transgenes. Therefore, the expression of the oncogenic transgene in H*ras*^{G12V} rats can be investigated using the LacZ541 reporter rat. In Hras/LacZ rats, immunostaining for LacZ revealed LacZ positive cells in the pancreas and these cells were clustered in ductal lesions (Fig. 4b). Because the cells expressing LacZ also express H*ras*^{G12V}, these results indicate that expression of oncogenic H*ras*^{G12V} gives rise to these lesions.

Until recently, a key genetic technology available for the mouse but not for the rat was the production of animals in which specified genes were disrupted (knockout animals) (Jacob and Kwitek, 2002). Pluripotent rat embryonic stem cell lines which are capable of producing genetically engineered rats have now been established (Buehr *et al.*, 2008; Kawamata and Ochiya, 2010; Li *et al.*, 2008). This crucial development, together with other recent advances in genetic engineering, such as the cloned rat (Zhou *et al.*, 2003), induced pluripotent stem (iPS) cells (Li *et al.*, 2009; Liao *et al.*, 2009), nucleases (ZFN/TALEN) (Geurts *et al.*, 2009; Tesson *et al.*, 2011; Tong *et al.*, 2012), and knockown/conditional knockdown by siRNA (Dann *et al.*, 2006), make genetically engineered rats powerful, innovative tools to advance biomedical research.

In conclusion, we have constructed a reporter line of rats that express LacZ only in cells expressing Cre recombinase and their daughter cells. The advantage of LacZ is the ease of visualization *in situ* and in section and whole mount preparations. The LacZ541 rat is an efficient and simple system for monitoring Cre expression and evaluating the performance of Cre-expressing systems which are based upon transgenic rats or somatic gene transfer vectors.

MATERIALS AND METHODS

Animals

For the generation of transgenic rats conditionally expressing LacZ, the CALNLZ switching unit was

obtained from Riken Bioresources Center DNA Bank (RDB1680) (Kanegae *et al.*, 1995), and the purified cassette was injected into the pronuclei of Sprague-Dawley rat zygotes (CLEA Japan, Tokyo, Japan). Techniques used for the generation of transgenic rats were the same as those reported previously (Asamoto *et al.*, 2000). A total of 313 injected eggs were transplanted into pseudo-pregnant Sprague-Dawley rats. Of 53 potential transgenic rats screened, 8 female rats were shown by PCR to carry the transgene. Transgenic founder rats were mated with Sprague-Dawley rats, and offspring were screened for the presence of the transgene by PCR analysis of genomic DNA isolated from tail biopsies at the age of 3 weeks. Homozygous transgenic rats were identified by semiquantitave PCR, and then confirmed by genetic testing.

Transgenic rats expressing Cre recombinase regulated by the CAG promoter (W-Tg(CAG-cre)81Jmsk) (NCre rat) were supplied by the National BioResource Project for the Rat in Japan (Kyoto, Japan, http://www.anim.med.kyoto-u.ac.jp/NBR/). Because the transgene is located on the X chromosome, homozygous female NCre rats were used in this study.

Male HA-K*ras*^{G12V} or H*ras*^{G12V} transgenic (Kras301 or Hras250) rats were established in our laboratory previously (Fukamachi *et al.*, 2009; Tanaka *et al.*, 2010; Ueda *et al.*, 2006).

All animal experiments were conducted according to the "Guidelines for Animal Experiments of the Nagoya City University Graduate School of Medical Sciences."

Detection of Recombination of the Transgene

Genomic DNA was extracted using standard methods (Laird *et al.*, 1991). Genomic DNA was used as the template for PCR reactions for detecting transgene recombination. The primers (Fig. 1, arrows) used were: 5′-CGTGCTGGTTGTTGTGCTGTCT-3′ (in the CAG promoter region), 5′-TCCTGTAGCCAGCTTTCATC-3′ (in the LacZ coding region).

X-Gal Staining

Transgene expression in NCre x LacZ541 progeny was determined by X-gal staining. Embryos or dissected tissues were fixed in 4% paraformaldehyde for 1 hr at 4°C, and then washed three times in rinse solution (2 mM $MgCl_2$, 0.01% sodium deoxycholate, 0.02% NP-40 in PBS). Specimens were treated with staining solution (1 mg ml^{-1} X-Gal, 5 mM $K_3[FeCN_6]$, 5 mM $K_4[FeCN_6]3H_2O$ in rinse solution) overnight (brain) or for 3 h (other organs) at 37°C.

Frozen sections were fixed in fixative solution (0.2% glutaraldehyde, 2 mM $MgCl_2$, 5 mM EGTA in PBS) for 5 min at 4°C, and then washed three times in rinse solution. Then they were treated with staining solution. The slides were counterstained with Kernechtrot solution (Nuclear fast red). After staining, samples were rinsed in distilled water three times, dehydrated with ethanol, cleared in xylene and mounted.

Cell Culture

Rat embryonic fibroblast cells (rEFs) were isolated from 14.5-day-postcoitum T_g rat embryos. Embryos were separated from maternal tissues and yolk sac and the internal organs were removed. The remaining tissues were finely minced and incubated with gentle agitation at 37°C for 10 min in 0.25% trypsin-EDTA. The cell suspension was then passed through an 18G needle and further incubated at 37°C for 15 min. The supernatant containing rEFs was plated in DMEM supplemented with 10% fetal bovine serum. The rEFs were fixed in formalin containing glutaraldehyde (2% formalin, 0.2% glutaraldehyde in PBS) for 5 min at 4°C. The fixed cells were treated with X-Gal staining solution at 37°C.

Tumor Induction, Immunohistochemistry and Immunofluorescence

Pancreas tumors were induced as described previously (Fukamachi *et al.*, 2009; Tanaka *et al.*, 2010; Ueda *et al.*, 2006). Briefly, purified adenovirus vector carrying Cre recombinase (AxCANCre) was injected into the pancreatic duct through the common bile duct. Animals were killed 3 weeks after injection of recombinant AxCANCre. Pathological examination was performed as described previously (Tanaka *et al.*, 2010). Paraffin section slides were treated with 0.1% trypsin for 20 min at 37°C and boiled for 10 min in citrate buffer before incubation with primary antibody: β-galactosidase (LacZ) antibody (AB9361, Abcam, Temecula, CA) diluted 1:100; HA-Tag antibody (6E2; Cell Signaling, Danvers, MA) diluted 1:100. Slides were incubated with secondary antibodies conjugated with Alexa Fluor488 (LacZ) and 546 (HA-Tag) (Molecular Probes, Eugene, OR). Nuclei were counterstained with TO-PRO-3 (Molecular Probes). Images were obtained with a FLUOVIEW FV300 confocal microscope (Olympus, Tokyo, Japan).

ACKNOWLEDGMENTS

The author thank Dr. T. Shirai (Nagoya City University) for assistance with histological examination, Dr. I. Saito (University of Tokyo) for the pCALNLZ plasmid, Dr. J. Miyazaki (Osaka University) for the CAG promoter, the National BioResource Project—Rat (http://www.anim.med.kyoto-u.ac.jp/NBR/) for providing rat strain.

LITERATURE CITED

Akagi K, Sandig V, Vooijs M, Van der Valk M, Giovannini M, Strauss M, Berns A. 1997. Cre-mediated somatic site-specific recombination in mice. Nucleic Acids Res 25:1766-1773.

Araki K, Araki M, Miyazaki J, Vassalli P. 1995. Site-specific recombination of a transgene in fertilized eggs by transient expression of Cre recombinase. Proc Natl Acad Sci USA 92:160–164.

Asamoto M, Ochiya T, Toriyama-Baba H, Ota T, Sekiya T, Terada M, Tsuda H. 2000. Transgenic rats carrying human c-Ha-ras proto-oncogenes are highly susceptible to *N*-methyl-*N*-nitrosourea mammary carcinogenesis. Carcinogenesis 21:243–249.

Buehr M, Meek S, Blair K, Yang J, Ure J, Silva J, McLay R, Hall J, Ying QL, Smith A. 2008. Capture of authentic embryonic stem cells from rat blastocysts. Cell 135:1287–1298.

Dann CT, Alvarado AL, Hammer RE, Garbers DL. 2006. Heritable and stable gene knockdown in rats. Proc Natl Acad Sci USA 103:11246–11251.

Feil R, Brocard J, Mascrez B, LeMeur M, Metzger D, Chambon P. 1996. Ligand-activated site-specific recombination in mice. Proc Natl Acad Sci USA 93:10887–10890.

Fukamachi K, Tanaka H, Hagiwara Y, Ohara H, Joh T, Iigo M, Alexander DB, Xu J, Long N, Takigahira M, Yanagihara K, Hino O, Saito I, Tsuda H. 2009. An animal model of preclinical diagnosis of pancreatic ductal adenocarcinomas. Biochem Biophys Res Commun 390:636–641.

Geurts AM, Cost GJ, Freyvert Y, Zeitler B, Miller JC, Choi VM, Jenkins SS, Wood A, Cui X, Meng X, Vincent A, Lam S, Michalkiewicz M, Schilling R, Foeckler J, Kalloway S, Weiler H, Menoret S, Anegon I, Davis GD, Zhang L, Rebar EJ, Gregory PD, Urnov FD, Jacob HJ, Buelow R. 2009. Knockout rats via embryo microinjection of zinc-finger nucleases. Science 325:433.

Inoue H, Ohsawa I, Murakami T, Kimura A, Hakamata Y, Sato Y, Kaneko T, Takahashi M, Okada T, Ozawa K, Francis J, Leone P, Kobayashi E. 2005. Development of new inbred transgenic strains of rats with LacZ or GFP. Biochem Biophys Res Commun 329:288–295.

Jacob HJ, Kwitek AE. 2002. Rat genetics: Attaching physiology and pharmacology to the genome. Nat Rev Genet 3:33–42.

Kanegae Y, Lee G, Sato Y, Tanaka M, Nakai M, Sakaki T, Sugano S, Saito I. 1995. Efficient gene activation in mammalian cells by using recombinant adenovirus expressing site-specific Cre recombinase. Nucleic Acids Res 23:3816–3821.

Kawamata M, Ochiya T. 2010. Generation of genetically modified rats from embryonic stem cells. Proc Natl Acad Sci USA 107:14223–14228.

Laird PW, Zijderveld A, Linders K, Rudnicki MA, Jaenisch R, Berns A. 1991. Simplified mammalian DNA isolation procedure. Nucleic Acids Res 19:4293.

Li P, Tong C, Mehrian-Shai R, Jia L, Wu N, Yan Y, Maxson RE, Schulze EN, Song H, Hsieh CL, Pera MF, Ying QL. 2008. Germline competent embryonic stem cells derived from rat blastocysts. Cell 135:1299–1310.

Li W, Wei W, Zhu S, Zhu J, Shi Y, Lin T, Hao E, Hayek A, Deng H, Ding S. 2009. Generation of rat and human induced pluripotent stem cells by combining genetic reprogramming and chemical inhibitors. Cell Stem Cell 4:16–19.

Liao J, Cui C, Chen S, Ren J, Chen J, Gao Y, Li H, Jia N, Cheng L, Xiao H, Xiao L. 2009. Generation of induced pluripotent stem cell lines from adult rat cells. Cell Stem Cell 4:11–15.

Rajewsky K, Gu H, Kuhn R, Betz UA, Muller W, Roes J, Schwenk F. 1996. Conditional gene targeting. J Clin Invest 98:600–603.

Sato Y, Endo H, Ajiki T, Hakamata Y, Okada T, Murakami T, Kobayashi E. 2004. Establishment of Cre/LoxP recombination system in transgenic rats. Biochem Biophys Res Commun 319:1197–1202.

Soriano P. 1999. Generalized lacZ expression with the ROSA26 Cre reporter strain. Nat Genet 21:70–71.

Tanaka H, Fukamachi K, Futakuchi M, Alexander DB, Long N, Tamamushi S, Minami K, Seino S, Ohara H, Joh T, Tsuda H. 2010. Mature acinar cells are refractory to carcinoma development by targeted activation of Ras oncogene in adult rats. Cancer Sci 101:341–346.

Tesson L, Usal C, Menoret S, Leung E, Niles BJ, Remy S, Santiago Y, Vincent AI, Meng X, Zhang L, Gregory PD, Anegon I, Cost GJ. 2011. Knockout rats generated by embryo microinjection of TALENs. Nat Biotechnol 29:695–696.

Tong C, Huang G, Ashton C, Wu H, Yan H, Ying QL. 2012. Rapid and cost-effective gene targeting in rat embryonic stem cells by TALENs. J Genet Genom 39:275–280.

Tsien JZ, Chen DF, Gerber D, Tom C, Mercer EH, Anderson DJ, Mayford M, Kandel ER, Tonegawa S. 1996. Subregion- and cell type-restricted gene knockout in mouse brain. Cell 87:1317–1326.

Ueda S, Fukamachi K, Matsuoka Y, Takasuka N, Takeshita F, Naito A, Iigo M, Alexander DB, Moore MA, Saito I, Ochiya T, Tsuda H. 2006. Ductal origin of pancreatic adenocarcinomas induced by conditional activation of a human Ha-ras oncogene in rat pancreas. Carcinogenesis 27:2497–2510.

Zhou Q, Renard JP, Le Friec G, Brochard V, Beaujean N, Cherifi Y, Fraichard A, Cozzi J. 2003. Generation of fertile cloned rats by regulating oocyte activation. Science 302:1179.

Carcinogenesis vol.34 no.6 pp.1251–1259, 2013
doi:10.1093/carcin/bgt053
Advance Access publication February 7, 2013

Metabolomic and transcriptomic profiling of human K-*ras* oncogene transgenic rats with pancreatic ductal adenocarcinomas

Setsuko Yabushita[1,*], Katsumi Fukamachi[2], Hajime Tanaka[3], Takako Fukuda[1], Kayo Sumida[1], Yoshihito Deguchi[1], Kazuki Mikata[1], Kazuhiko Nishioka[1], Satoshi Kawamura[1], Satoshi Uwagawa[1], Masumi Suzui[2], David B.Alexander[2,4] and Hiroyuki Tsuda[4]

[1]Environmental Health Science Laboratory, Sumitomo Chemical Co., Osaka 554-8558, Japan, [2]Department of Molecular Toxicology, Nagoya City University Graduate School of Medical Sciences, Nagoya 467-8601, Japan, [3]Department of Gastroenterology and Metabolism, Nagoya City University Graduate School of Medical Sciences, Nagoya 467-8601, Japan and [4]Nanotoxicology Project, Nagoya City University, Nagoya 467-8603, Japan

*To whom correspondence should be addressed. Tel: +81-66466-5306; Fax: +81-66466-5319;
Email: yabushitas@sc.sumitomo-chem.co.jp

Pancreatic ductal adenocarcinoma (PDAC) is one of the most debilitating malignancies in humans, and one of the reasons for this is the inability to diagnose this disease early in its development. To search for biomarkers that can be used for early diagnosis of PDAC, we established a rat model of human PDAC in which expression of a human K-*rasG12V* oncogene and induction of PDAC are regulated by the *Cre/lox* system. In the present study, transgenic rats bearing PDAC and control transgenic rats with normal pancreatic tissues were used for metabolomic analysis of serum and pancreatic tissue by non-targeted and targeted gas chromatography–mass spectrometry and transcriptomic analysis of pancreatic tissue by microarray. Comparison of the metabolic profiles of the serum and pancreatic tissue of PDAC-bearing and control rats identified palmitoleic acid as a metabolite, which was significantly decreased in the serum of PDAC-bearing animals. Transcriptomic analysis indicated that several transcripts involved in anaerobic glycolysis and nucleotide degradation were increased and transcripts involved in the trichloroacetic acid cycle were decreased. Other transcripts that were changed in PDAC-bearing rats were adenosine triphosphate citrate lyase (decreased: fatty acid biosynthesis), fatty acid synthase (increased: fatty acid biosynthesis) and arachidonate 5-lipoxygenase activating protein (increased: arachidonic acid metabolism). Overall, our results suggest that the decreased serum levels of palmitoleic acid in rats with PDAC was likely due to its decrease in pancreatic tissue and that palmitoleic acid should be investigated in human samples to assess its diagnostic significance as a serum biomarker for human PDAC.

Introduction

Pancreatic cancer is diagnosed in ~1 person per 10 000 annually in the USA and is the fifth leading cause of cancer mortality. Most patients die within 1 year of diagnosis, and the 5 year survival rate, less than 5%, is dismal (1). Pancreatic ductal adenocarcinomas (PDACs) are diagnosed in ≥95% of the patients with pancreatic cancer. The most widely used marker for pancreatic cancer, CA19-9, lacks specificity and sensitivity: it is elevated in cases of benign cholangitis and pancreatitis and also in other types of cancer, and it is not elevated during the early stages of PDAC, when the lesion is potentially curable (2–4). Thus, there are presently no reliable biomarkers for the early detection of pancreatic cancer. Consequently, there is an urgent need for specific and sensitive biomarkers of pancreatic cancer.

Previously, we established transgenic rats in which expression of the human H-*ras*^{G12V} or K-*ras*^{G12V} oncogene is regulated by the *Cre/lox* system (5). Targeted activation of H-*ras*^{G12V} or K-*ras*^{G12V} is accomplished by injection of a *Cre*-carrying adenovirus into the pancreatic ducts through the common bile duct. Several weeks after injection, proliferative lesions in pancreatic duct epithelium, intercalated ducts and centroacinar cells, but not acinar cells, become widespread. The histopathological appearance of these adenocarcinomas closely resembles that described for typical pancreatic tumors in man. Thus, transgenic rats with induced PDACs in pancreatic tissues are an appropriate model for human PDAC. In this study, K-*ras*^{G12V} transgenic rats (K-*ras*^{G12V} Tg rats) were used because K-*ras* mutations are commonly observed in human PDAC.

Serum/plasma biomarkers are ideal in that the collection of samples is relatively non-invasive, and samples can be obtained repeatedly to monitor disease progression. Molecular profiling approaches such as transcriptomics, proteomics and metabolomics to monitor pathological processes of disease have received a great deal of attention. Metabolomic analysis refers to the comprehensive study of the many metabolites present in biological samples (6,7). The analytical techniques typically applied are nuclear magnetic resonance (8) and mass spectrometry (9), with the latter being coupled to chromatographic separation techniques such as gas chromatography or liquid chromatography. Metabolomics is a powerful method for screening biomarkers, interpreting biological pathways and understanding functions of complex biological systems (10). Recently, a urinary biomarker of prostate cancer aggressiveness was found using metabolomic profiling (11).

In the present study, we characterized the metabolite profiles of both serum and pancreatic tissue samples from control and PDAC-bearing K-*ras*^{G12V} Tg rats by non-targeted and targeted gas chromatography–mass spectrometry (GC-MS) analysis to identify potential serum biomarkers for the clinical diagnosis of PDAC. In addition, the metabolomic analysis was integrated with a transcriptomic analysis of pancreatic tissues to obtain a better understanding of the behavior of metabolites in PDAC. We identified palmitoleic acid as a metabolite that was significantly decreased in the serum of rats with PDAC, and integrated metabolomic and transcriptomic analyses suggest fluctuations in several metabolomic pathways in PDAC lesions.

Abbreviations: Acly, adenosine triphosphate citrate lyase; Alox5ap, arachidonate 5-lipoxygenase activating protein; Fasn, fatty acid synthase; GC-MS, gas chromatography–mass spectrometry, PCA, principal component analysis; PDAC, pancreatic ductal adenocarcinoma; TCA, trichloroacetic acid; TIC, total ion current.

Materials and methods

Ethics statement

All experiments were conducted in accordance with the 'Guidelines for Animal Experiments of Nagoya City University Graduate School of Medical Sciences', and the experimental protocol was approved by the Nagoya City University Medical School Institutional Animal Care and Use Committee.

Induction of pancreatic ductal adenocarcinoma

Kras301 rats conditionally expressing human K-*ras*^{G12V} were generated as described previously (12). An adenovirus vector carrying the *Cre* gene (AxCANCre) and an empty adenovirus vector (AxCAwt) were injected into the pancreatic ducts of 10–11-week-old adult homozygous male Kras301 rats through the common duct as described previously (5,12). Six rats were treated with AxCANCre (PDAC rats) and four with AxCAwt (as controls). All rats were maintained in plastic cages in an air-conditioned room with a 12 h light/12 h dark cycle and euthanized by blood withdrawal from the abdominal aorta under anesthesia 16–17 days after the injection of adenovirus vector.

Collection of pancreatic tissue and serum

Rats were killed by exsanguination under ether anesthesia. Immediately after exsanguination, pancreatic tissues were excised from euthanized rats, cut into portions and the portions either frozen in liquid nitrogen or processed for

pathological examination (see below). Collected blood samples were allowed to clot at room temperature and then centrifuged at 3000 r.p.m. for 10 min at 4°C to obtain serum. The frozen pancreatic tissues and the serum were stored in liquid nitrogen and at −80°C, respectively, until metabolomic analysis.

Pathological examination

The remaining pancreatic tissues from PDAC and control rats were fixed in 4% paraformaldehyde, processed for embedding in paraffin, cut into 3 μm sections and stained with hematoxylin and eosin for microscopic examination.

RNA extraction from pancreatic tissues

Extraction of total RNA was performed using an RNeasy Mini Kit (Qiagen, Hilden, Germany). Quantification was performed with an Amersham Pharmacia spectrophotometer, model Ultraspec 3100pro (Amersham Pharmacia Biotech, Uppsala, Sweden), and assessment of ribosomal RNA integrity was performed using a 2100 Bioanalyzer (Agilent Technologies, Palo Alto, CA). Total RNA samples were stored at −80°C immediately after extraction.

Gene expression analysis

Gene expression levels were measured using a GeneChip System (Affymetrix, Santa Clara, CA). Reverse transcription of the extracted total RNA, second-strand synthesis and probe generation were all accomplished with One-Cycle Target Labeling and Control Reagents (Affymetrix) following the manufacturer's protocol. Briefly, from 5 μg of total RNA, first-strand cDNA was synthesized with SuperScript II reverse transcriptase and a T7-oligo (dT) primer, and double-strand cDNA was synthesized with *Escherichia coli* RNase H, *E.coli* DNA polymerase I and *E.coli* DNA ligase. Biotin-labeled cRNA was prepared from the double-strand cDNA, and 15 μg of labeled cRNA was fragmented. Rat Genome 230 2.0 arrays were hybridized as described in the Gene Chip Expression Analysis Technical Manual (Affymetrix). The arrays were stained and washed with R-Phycoerythrin Streptavidin (Molecular Probes, Eugene, OR) and with the GeneChip Hybridization, Wash, and Stain Kit (Affymetrix). Fluorescence was intensified by the antibody-amplification method. The arrays were scanned with a GeneChip Scanner 3000 (Affymetrix) with Affymetrix Genechip Command Console (AGCC) and the image files were analyzed with an Affymetrix data suite system, Expression Console (EC) version 1.1; the tab-delimited files obtained contained data regarding the relative levels of expression of transcripts (signal) and the reliability of detection (Detection Call). The derived signal values were globally normalized to 100.

Sample preparation for GC-MS analysis

Pancreatic tissue and serum were subjected to two derivatization steps for GC-MS analysis. Pancreatic tissue samples (45–84 mg) were weighed and homogenized in a 12-fold volume solution of methanol/water/10 mM 2-hydroxyundecanoic acid (800:100:1, v/v/v; 10 mM 2-hydroxyundecanoic acid was used as an internal standard) using a potter homogenizer on ice, followed by centrifugation at 15 000 r.p.m. for 10 min at 4°C. Serum samples (50 μl) were deproteinized by addition of an 8-fold volume solution of methanol/water/10 mM 2-hydroxyundecanoic acid (800:100:1, v/v/v; 10 mM 2-hydroxyundecanoic acid was used as an internal standard), followed by centrifugation at 15 000 r.p.m. for 5 min at 4°C. The supernatant (200 μl) was dried in a vacuum freeze dryer, 30 μl of methoxylamine hydrochloride (Sigma–Aldrich) in pyridine (10 mg/ml) was added as a derivatizing agent and the mixture was incubated at 30°C for 90 min. Thereafter, 30 μl of *N*-methyl-*N*-(trimethylsilyl)trifluoroacetamide (GL Science, Tokyo, Japan) was added for derivatization, and the mixture was incubated at 40°C for 30 min.

GC-MS analysis

All analyses were carried out with a Bruker Daltonics1200 GC/MS/MS system (Bruker Daltonics K.K., Japan) using an Agilent Technologies VF5-ms capillary column (length, 30 m; internal diameter, 0.25 mm; film thickness, 0.25 μm). The injection temperature was 230°C. The helium gas flow rate through the column was 1 ml/min. The column oven temperature was 60°C for 2 min and rose at 10°C/min to 300°C and then remained at 300°C for 5 min. Ions were generated at an electron impact energy of 70 kV and were recorded over the mass range from *m/z* 70 to 800.

Analysis of GC-MS data

GC-MS data were imported into LineUp (Infometrix, Bothell, WA) and PiroTrans (GL Science) in order to align the chromatogram on the basis of peak intensity and the retention time of the internal standard, 2-hydroxyundecanoic acid. The generated peak lists were imported into Pirouette software (Infometrix, Woodinville, WA) for multivariate statistical analysis. Principal component analysis (PCA) was conducted to find discriminatory metabolites in serum and pancreatic tissues of PDAC rats. Identification of discriminatory metabolites detected by PCA analysis was performed using the NIST 05 Mass Spectral Library (NIST) containing >200 000 electron impact spectra. In addition to the automatic library search assessment on the basis of similarity score (>65), the similarity of spectra was manually confirmed.

Identification and quantification of palmitoleic acid in pancreatic tissues

To authenticate the identity of the metabolite putatively identified as palmitelaidic acid, pancreatic tissues were analyzed by cochromatography with palmitelaidic acid and palmitoleic acid standards (MP Biomedicals, CA). The identity of the metabolite was determined based on comparison of the retention time and fragment pattern of the metabolite and those of the two standards.

For concentration measurements, palmitoleic acid was diluted in pyridine and six standards of various mixtures of compounds of known concentration between 0.05 and 100 p.p.m. were prepared. The concentration of palmitoleic acid in the samples was quantified by a standard curve of total ion current (TIC) chromatograms or *m/z* 311 mass chromatograms.

Statistics

The peak intensities of metabolites and the signal values of gene expression were statistically analyzed by the Student's *t*-test between PDAC and control rats, with a level of probability of 0.05 used as the criterion for significance.

Results

Gross and histological observation

Kras301 rats, 13–14 weeks of age, were killed 16–17 days after injection of adenovirus vector into the pancreatic duct via the common bile duct. Gross and histological findings were the same as reported previously (5,12,13). PDAC was well developed with grossly visible whitish lesions in all six rats treated with AxCANCre. Histopathological examination showed that the tumors were adenocarcinomas with a variable amount of fibrotic tissue, some showing desmoplastic morphology and infiltration of inflammatory cells. Invasion of the surrounding normal pancreatic tissue by the PDAC that developed in Kras301 rats was a common feature of these lesions. Figure 1 shows typical lesions that developed in the Kras301 rats.

PDAC that develop in Kras301 rats are not metastatic, and neoplastic lesions were not found in any other organs. No abnormalities were observed in pancreatic tissues of the four rats injected with AxCAwt.

GC-MS chromatograms of serum and pancreatic tissues

Typical GC-MS TIC chromatograms of serum and pancreatic tissue extracts are shown in Supplementary Figure 1, available at *Carcinogenesis* Online. The retention time of the internal standard was consistent for each run. The data showed marked differences in the chromatogram patterns between the serum and pancreatic tissue.

Clustering of control and PDAC samples

Score plots produced by PCA of the serum pancreatic tissue are shown in Figure 2. The PCA algorithm generates a single point that represents the metabolites in a sample and their concentrations (each dot in the score plots shown in Figure 2 represents a single rat); close clustering of dots indicates that the samples have similar compositions. The control and PDAC samples clustered into two distinct groups in both the serum (Figure 2A) and pancreatic tissue (Figure 2B) score plots, indicating that the profiles of the metabolites in the serum and pancreatic tissue samples derived from the control rats differed from those derived from the rats with PDAC.

Metabolite differences between control and PDAC samples screened by PCA

In addition to the score plot, which is based on the composition of the samples, the PCA algorithm also creates a loading plot, which is based on metabolite values. Loading plots identify metabolites that contribute to the differential clustering of PDAC and control samples in the score plots. The electron impact spectra of these discriminatory metabolites were then compared with the NIST 05 Mass Spectral Library (NIST). Putatively identified discriminatory metabolites with matching NIST spectra are shown in Table I. Fold changes and *P*-values of these metabolites in the serum and pancreatic tissues were calculated by the TICs of GC-MS chromatograms.

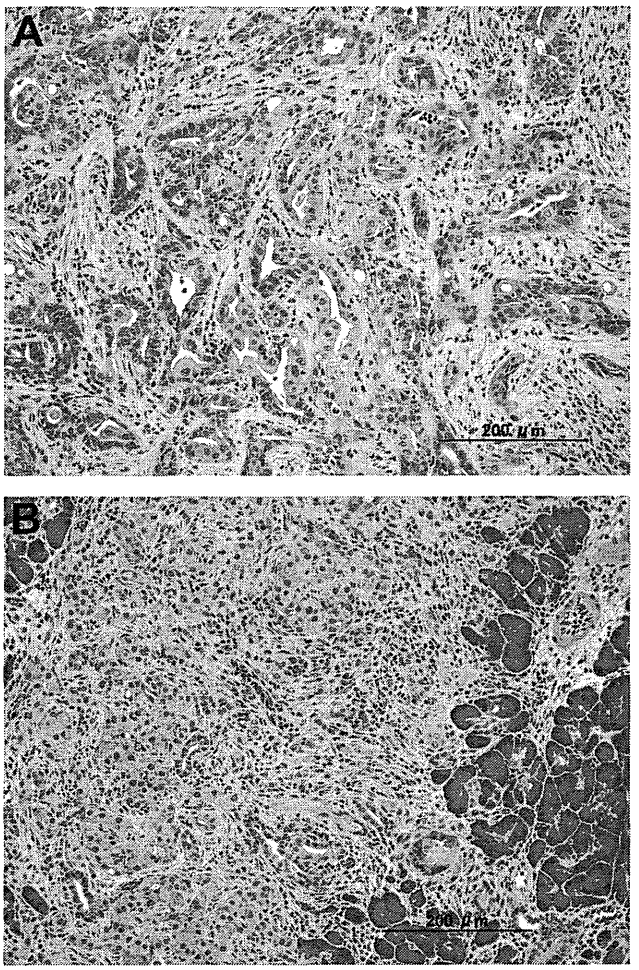

Fig. 1. Typical lesions that developed in the Kras301 rats are shown. (**A**) An adenocarcinoma with desmoplastic appearance. (**B**) An adenocarcinoma invading the surrounding pancreas tissue.

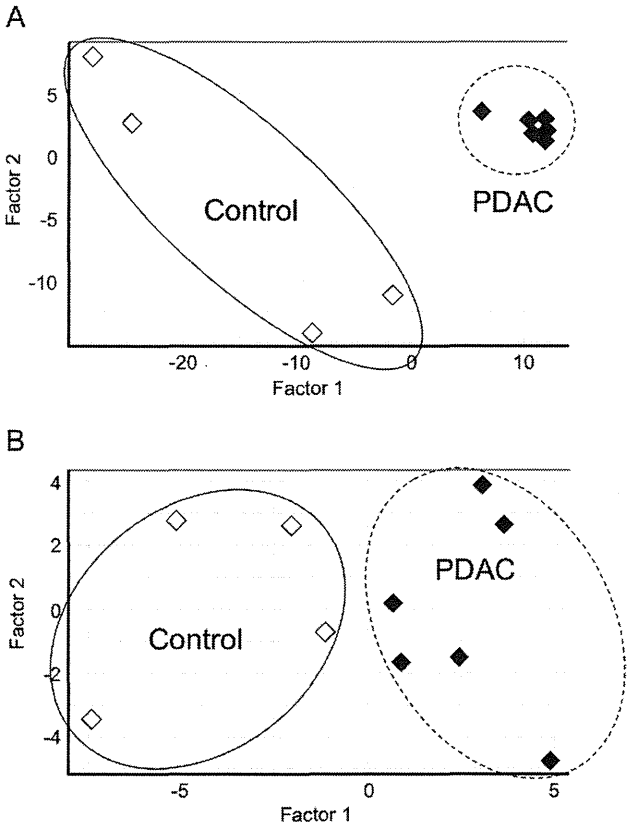

Fig. 2. Score plots of PCA based on the metabolite profile data of PDAC rats and control rats. The rhombus plots (filled and open) indicate the results for PDAC rats ($n = 6$) and control rats ($n = 4$), respectively. (**A**) Score plots of PCA based on the metabolite profile data for pancreatic tissues discriminating between PDAC and control rats. The principal components PC1 ($t[1]$) and PC2 ($t[2]$) described 59.6 and 14.9% of the variation. (**B**) Score plots of PCA based on the metabolite profile data of serum discriminating between PDAC and control rats. The principal components PC1 ($t[1]$) and PC2 ($t[2]$) described 32.8 and 18.0% of the variation.

In the serum, aminomalonic acid, 2-aminoethyl dihydrogen phosphate, citrate and lanthionine were significantly increased and chenodeoxycholic acid was non-significantly increased (1.9-fold). In pancreatic tissues, however, none of these metabolites was significantly increased and aminomalonic acid was significantly decreased.

A number of fatty acids were decreased in pancreatic tissues: palmitelaidic acid, linoleic acid, octadecanoic acid, myristic acid, arachidonic acid and hexadecanoic acid were significantly decreased and tridecanoic acid, 12-methyl-, methyl ester and heptadecanoic acid were non-significantly decreased. Of these fatty acids, only palmitelaidic acid (significantly decreased) and arachidonic acid (non-significantly decreased) were also decreased in the serum.

A third metabolite that had corresponding fluctuations in both the serum and pancreatic tissue was 2(1*H*)-pyrimidinone. This metabolite was significantly decreased in pancreatic tissues and non-significantly in the serum.

None of the other discriminatory metabolites had corresponding fluctuations in both the serum and pancreatic tissue. Beta-alanine, xanthine and uridine were increased in pancreatic tissue but not in the serum, and aspartic acid, alpha-glycerophosphoric acid, tyrosine, 2-monopalmitin, adenosine monophosphate and purine were decreased in pancreatic tissue but not in the serum.

Overall, the metabolic profiles in the pancreatic tissue and the serum of control and PDAC-bearing rats were different, with several discriminatory metabolites contributing to this difference. The array of changes in the individual discriminatory metabolites in the serum and pancreatic tissue, however, were distinct.

Identification and quantification of palmitoleic acid in pancreatic tissue and serum using standard chemicals

Once a metabolite that was significantly decreased in both pancreatic tissues and serum was detected and putatively identified as palmitelaidic acid, the identification of the metabolite was authenticated by cochromatography with palmitelaidic acid and palmitoleic acid. The retention time and fragment pattern of the standards identified the putatively annotated palmitelaidic acid as 'palmitoleic acid'.

A standard curve was then used for concentration measurement in samples: the linear region of quantitation was between 0.1 and 100 p.p.m. ($R^2 = 0.9857$). The concentrations of palmitoleic acid in pancreatic tissues and serum of the individual control and PDAC-bearing rats are shown in Table II. The palmitoleic acid concentration in the pancreatic tissues of control and PDAC rats was 266.5 186.2 and 7.5 4.6 p.p.m., respectively, and the concentration of palmitoleic acid in the serum samples of control and PDAC-bearing rats was 2.6 0.8 and 1.2 0.1 p.p.m., respectively (P-value: 0.031).

Alternations in the levels of metabolites involved in glycolysis and the trichloroacetic acid cycle

The 'Warburg effect' in which tumor cells rapidly use glucose and convert the majority of it to lactate is known as a typical signature of cancer (14,15). Since we observed decreases for a number of fatty acids, which are functionally related to the glycolytic pathway, in the pancreatic tissue of PDAC-bearing rats, we searched for peaks

Table I. Fold changes of the discriminatory metabolites characterizing PDAC tissues and serum

Metabolites	Retention time (min)	Serum		Pancreatic tissues	
		PDAC/control		PDAC/control	
		Fold changes	*P*-values	Fold changes	*P*-values
Threonine	10.37	1.2[a]	0.373	1.3	0.330
Beta-alanine	10.94	ND		1.7[a]	0.072
Aminomalonic acid	11.46	1.3	0.011*	0.8[a]	0.019*
Aspartic acid	12.07	1.3	0.106	0.7[a]	0.005*
Tridecanoic acid, 12-methyl-, methyl ester	14.53	ND		0.1[a]	0.051
Alpha-glycerophosphoric acid	14.79	1.4	0.060	0.8[a]	0.000*
2-Aminoethyl dihydrogen phosphate	15.04	1.2[a]	0.035*	1.0	0.257
Citrate	15.40	1.3[a]	0.017*	1.2	0.522
Tyrosine	16.67	1.2	0.086	0.3[a]	0.024*
Xanthine	17.45	1.1	0.405	1.7[a]	0.016*
Palmitelaidic acid	17.54	0.6[a]	0.002*	0.1[a]	0.001
Heptadecanoic acid	18.62	0.9	0.277	0.3[a]	0.062
Linoleic acid	19.24	0.9	0.683	0.2[a]	0.000*
Octadecanoic acid	19.57	ND		0.7[a]	0.001*
Lanthionine	19.87	1.4[a]	0.027*	1.0	0.949
Myristic acid	20.46	0.9	0.138	0.1[a]	0.020*
Arachidonic acid	20.56	0.4[a]	0.098	0.6[a]	0.021*
Uridine	21.22	ND		3.2[a]	0.001*
2-Monopalmitin	21.97	1.0	0.205	0.05[a]	0.001*
Hexadecanoic acid	22.22	0.9	0.203	0.1[a]	0.038*
2(1*H*)-Pyrimidinone	23.96	0.5	0.316	0.5[a]	0.000*
Adenosine monophosphate	25.55	0.9	0.304	0.5[a]	0.000*
Purine	25.85	ND		0.4[a]	0.000*
Chenodeoxycholic acid	27.14	1.9[a]	0.148	1.1	0.643

Sera and pancreatic tissues from PDAC rats ($n = 6$) and controls ($n = 4$) were analyzed. ND, peaks were not detected.
[a]Metabolites that contributed to the differentiation of PDAC and control samples in the PCA analysis.
*$P < 0.05$.

Table II. Concentration of palmitoleic acid in the tissue and serum of control and PDAC rats

Rat no.	Concentration in tissue or serum (p.p.m.[a])		*t*-Test
Pancreas control			
30	347.72	266.5±186.2	
38	490.90		
50	127.08		
83	100.33		
Pancreas PDAC			
42	10.58	7.5±4.6	0.069
47	2.01		
84	3.78		
86	13.77		
87	4.97		
88	10.18		
Serum control			
30	2.77	2.6±0.8	
38	3.65		
50	1.97		
83	2.10		
Serum PDAC			
42	1.15	1.2±0.1	0.031
47	0.96		
84	1.34		
86	1.28		
87	1.09		
88	1.20		

[a]p.p.m. in tissue is microgram palmitoleic acid per gram tissue and p.p.m. in serum is microgram palmitoleic acid per milliliter serum.

of metabolites involved in glycolysis and the trichloroacetic acid (TCA) cycle. Glucose, pyruvate, lactate, succinate, fumarate, malate and alph-keto-glutarate were identified. The changes in the levels of these metabolites in the serum and pancreatic tissues were calculated by the TICs of GC-MS chromatograms (Table III). No significant differences between PDAC-bearing rats and control rats were found.

Transcriptional changes related to glycolysis, TCA cycle, fatty acid biosynthesis, arachidonic acid metabolism and nucleotide degradation

Transcriptional data for ~31 000 genes in PDAC and control pancreatic tissue were analyzed by microarray; the genes for which significant changes ($P \leq 0.05$) occurred are shown in Supplementary Table 1, available at *Carcinogenesis* Online. Values for enzymes involved in glycolysis, the TCA cycle, fatty acid biosynthesis, arachidonic acid metabolism and nucleotide degradation are shown in Table IV. Changes in Abat, Alox5, Dpyd, Dpys, Nt5, Uox and Upb transcription were evaluated as unclear as their expression levels were too low to be analyzed accurately by microarray analysis.

Pathways generated by integrating the results we obtained from our metabolic and transcriptional analyses are shown in Figure 3. In PDAC lesions, numerous transcripts involved in anaerobic glycolysis were upregulated and most of those involved in the TCA cycle were downregulated (Figure 3A). Transcription of two lipogenic enzymes was also changed in PDAC lesions: adenosine triphosphate citrate lyase (Acly) was decreased and fatty acid synthase (Fasn) was increased (Figure 3A).

Transcripts of arachidonate 5-lipoxygenase activating protein (Alox5ap), which is necessary for activation of Alox5, were increased (Figure 3B). This increase may be associated with the decrease of linoleic acid and arachidonic acid found in the pancreatic tissue of PDAC-bearing rats (Table I).

A number of transcripts involved in purine and pyrimidine nucleotide degradation were increased; however, transcripts involved in pyrimidine nucleotide degradation downstream of beta-alanine degradation were decreased (Figure 3C). Taken together, these changes may be associated with the changes of adenosine monophosphate, xanthine, uridine and beta-alanine found in pancreatic tissue of PDAC-bearing rats.

Table III. Fold changes of the putatively identified metabolites related to glycolysis and the TCA cycle

Metabolites	Retention time (min)	Serum		Pancreatic tissues	
		PDAC/control		PDAC/control	
		Fold changes	*P*-values	Fold changes	*P*-values
Glucose	16.17	1.0	0.510	1.0	0.940
Pyruvate	5.87	1.1	0.177	1.0	0.198
Lactate	5.95	1.0	0.456	1.0	0.373
Succinate	9.46	0.6	0.065	1.1	0.693
Fumarate	9.62	1.1	0.144	ND	
Malate	11.67	0.9	0.803	0.7	0.054
Alpha-ketoglutarate	12.75	1.0	0.832	0.8	0.631

Sera and pancreatic tissues from PDAC rats ($n = 6$) and controls ($n = 4$) were analyzed. ND, not detected.

Table IV. Microarray analysis of mRNA from pancreatic tissues from control and PDAC rats

Gene symbol	Representative public ID	Gene title	Fold	*P*-value
Abat	U29701	4-Aminobutyrate aminotransferase	0.0	0.077[a]
Acly	NM_016987	Adenosine triphosphate citrate lyase	0.6	0.000*
Aco2	NM_024398	Aconitase 2, mitochondrial	0.6	0.000*
Ada	NM_130399	Adenosine deaminase	3.9	0.000*
Adar	NM_031006	Adenosine deaminase, RNA-specific	0.4	0.018*
Adar	BI292196	Adenosine deaminase, RNA-specific	0.8	0.408
Adarb1	NM_012894	Adenosine deaminase, RNA-specific, B1	0.6	0.294
Adarb1	AW253867	Adenosine deaminase, RNA-specific, B1	0.1	0.066
Adarb1	AW522471	Adenosine deaminase, RNA-specific, B1	3.4	0.000*
Adarb2	NM_133302	Adenosine deaminase, RNA-specific, B2	3.3	0.012*
Adat3	AI029510	Adenosine deaminase, tRNA-specific 3, TAD3 homolog (*S. cerevisiae*)	0.4	0.139
Aldh6a1	NM_031057	Aldehyde dehydrogenase 6 family, member A1	0.2	0.001*
Aldoa	NM_012495	Aldolase A, fructose bisphosphate	4.0	0.001*
Aldob	M10149	Aldolase B, fructose bisphosphate	0.0	0.146
Aldoc	NM_012497	Aldolase C, fructose bisphosphate	0.6	0.100
Alox5	NM_012822	Arachidonate 5-lipoxygenase	2.1	0.081[a]
Alox5ap	NM_017260	Arachidonate 5-lipoxygenase activating protein	3.0	0.000*
Ampd1	J02811	Adenosine monophosphate deaminase 1 (isoform M)	0.8	0.707
Ampd2	BE111787	Adenosine monophosphate deaminase 2 (isoform L)	0.7	0.029*
Ampd2	BE100752	Adenosine monophosphate deaminase 2 (isoform L)	1.5	0.068
Ampd3	NM_031544	Adenosine monophosphate deaminase 3	2.6	0.006*
Cda	AA859352	Cytidine deaminase	2.7	0.031*
Cs	NM_130755	Citrate synthase	1.1	0.119
Cs	AI009657	Citrate synthase	1.2	0.020*
Cs	H33235	Citrate synthase	1.3	0.013*
Dpyd	NM_031027	Dihydropyrimidine dehydrogenase	0.2	0.106[a]
Dpys	NM_031705	Dihydropyrimidinase	0.0	0.377[a]
Eno1	NM_012554	Enolase 1 (alpha)	3.7	0.000*
Eno2	AF019973	Enolase 2 (gamma), neuronal	5.9	0.000*
Eno3	NM_012949	Enolase 3, beta, muscle	0.7	0.457
Fasn	NM_017332	Fatty acid synthase	0.8	0.433
Fasn	AI179334	Fatty acid synthase	2.1	0.000*
Fh1	NM_017005	Fumarate hydratase 1	0.9	0.355
Gapdh	AFFX_Rat_GAPDH_3	Glyceraldehyde-3-phosphate dehydrogenase	3.0	0.001*
Gapdh	AFFX_Rat_GAPDH_5	Glyceraldehyde-3-phosphate dehydrogenase	2.7	0.003*
Gapdh	AFFX_Rat_GAPDH_M	Glyceraldehyde-3-phosphate dehydrogenase	2.6	0.003
Gapdh /// Gapdh-ps2	NM_017008	Glyceraldehyde-3-phosphate dehydrogenase /// glyceraldehyde-3-phosphate dehydrogenase, pseudogene 2	4.0	0.001*
Gck	NM_012565	Glucokinase	0.3	0.152
Gda	AF245172	Guanine deaminase	3.8	0.001*
Got1	D00252	Glutamic-oxaloacetic transaminase 1, soluble (aspartate aminotransferase 1)	1.1	0.589
Got2	NM_013177	Glutamic-oxaloacetic transaminase 2, mitochondrial (aspartate aminotransferase 2)	2.1	0.002*
Got2 /// LOC297793 /// LOC314123	BI296539	Glutamic-oxaloacetic transaminase 2, mitochondrial (aspartate aminotransferase 2) /// similar to aspartate aminotransferase, mitochondrial precursor (transaminase A) (glutamate oxaloacetate transaminase 2) /// similar to aspartate aminotransferase, mitochondrial precursor (transaminase A) (glutamate oxaloacetate transaminase 2)	1.6	0.029*
Gpd1	NM_022215	Glycerol-3-phosphate dehydrogenase 1 (soluble)	1.3	0.737

Table IV. *Continued*

Gene symbol	Representative public ID	Gene title	Fold	*P*-value
Gpd1	BI277042	Glycerol-3-phosphate dehydrogenase 1 (soluble)	0.3	0.048*
Gpi	BI283882	Glucose phosphate isomerase	3.9	0.000*
Gpt	NM_031039	Glutamic-pyruvate transaminase (alanine aminotransferase)	0.1	0.009*
Hk1	NM_012734	Hexokinase 1	0.8	0.476
Hk1	AFFX_Rat_Hexokinase_3	Hexokinase 1	2.4	0.056
Hk1	AFFX_Rat_Hexokinase_5	Hexokinase 1	0.8	0.559
Hk1	AFFX_Rat_Hexokinase_M	Hexokinase 1	0.7	0.319
Hk2	NM_012735	Hexokinase 2	1.3	0.366
Hk2	BI294137	Hexokinase 2	1.8	0.001*
Hprt1	M86443	Hypoxanthine phosphoribosyltransferase 1	1.3	0.047*
Idh2	AI172491	Isocitrate dehydrogenase 2 ($NADP^+$), mitochondrial	0.5	0.000*
Idh3a	NM_053638	Isocitrate dehydrogenase 3 (NAD^+) alpha	2.3	0.001*
Idh3B	AI171793	Isocitrate dehydrogenase 3 (NAD^+) beta	0.7	0.000*
Idh3g	BI277627	Isocitrate dehydrogenase 3 (NAD), gamma	0.6	0.001*
Ldha	NM_017025	Lactate dehydrogenase A	2.6	0.004*
Ldhb	AA848319	Lactate dehydrogenase B	2.3	0.005*
Ldhc	NM_017266	Lactate dehydrogenase C	0.4	0.334
Ldhd	AI145761	Lactate dehydrogenase D	0.7	0.380
Ldhd	AI501131	Lactate dehydrogenase D	0.4	0.051
Mdh1	NM_033235	Malate dehydrogenase 1, NAD (soluble)	0.6	0.003*
Mdh1	BG671530	Malate dehydrogenase 1, NAD (soluble)	0.6	0.004*
Mdh2	NM_031151	Malate dehydrogenase 2, NAD (mitochondrial)	0.6	0.009
Me1	M30596	Malic enzyme 1, NADP(+)-dependent, cytosolic	3.1	0.003*
Me1	NM_012600	Malic enzyme 1, NADP(+)-dependent, cytosolic	2.0	0.035*
Nt5c3	AI409146	5′-Nucleotidase, cytosolic III	0.8	0.151
Nt5c3l	BF412799	5′-Nucleotidase, cytosolic III like	0.9	0.360
Nt5e	NM_021576	5′-Nucleotidase, ecto	1.1	0.745
Nt5e	BI289470	5′-Nucleotidase, ecto	1.1	0.696
Nt5m	AA819763	5′,3′-Nucleotidase, mitochondrial	2.6	0.052
Ogdh	BI277513	Oxoglutarate (alpha-ketoglutarate) dehydrogenase (lipoamide)	1.3	0.004*
Ogdh	BE103050	Oxoglutarate (alpha-ketoglutarate) dehydrogenase (lipoamide)	1.0	0.968
Pc	NM_012744	Pyruvate carboxylase	0.4	0.016*
Pdha1	AI411413	Pyruvate dehydrogenase (lipoamide) alpha 1	0.7	0.005*
Pdha1	BF561717	Pyruvate dehydrogenase (lipoamide) alpha 1	0.5	0.006*
Pdha2	NM_053994	Pyruvate dehydrogenase (lipoamide) alpha 2	0.1	0.302
Pdhb	BM389223	Pyruvate dehydrogenase (lipoamide) beta	0.4	0.001*
Pfkl	NM_013190	Phosphofructokinase, liver	1.0	0.952
Pfkm	NM_031715	Phosphofructokinase, muscle	0.8	0.001*
Pfkm	AI071717	Phosphofructokinase, muscle	0.3	0.143
Pfkm	BI291434	Phosphofructokinase, muscle	0.4	0.165
Pfkp	BM389769	Phosphofructokinase, platelet	3.5	0.001*
Pgam1	NM_053290	Phosphoglycerate mutase 1 (brain)	1.8	0.004*
Pgam2	NM_017328	Phosphoglycerate mutase 2 (muscle)	0.7	0.287
Pgk1	NM_053291	Phosphoglycerate kinase 1	0.3	0.131
Pgk1	NM_053291	Phosphoglycerate kinase 1	3.4	0.005*
Pgk1	BI279760	Phosphoglycerate kinase 1	2.2	0.011*
Pklr	NM_012624	Pyruvate kinase, liver and RBC	0.1	0.207
Pklr	M17685	Pyruvate kinase, liver and RBC	0.3	0.273
Pkm2	NM_053297	Pyruvate kinase, muscle	7.7	0.001*
Sdha	NM_130428	Succinate dehydrogenase complex, subunit A, flavoprotein (Fp)	0.8	0.009*
Sdhb	AI172320	Succinate dehydrogenase complex, subunit B, iron sulfur (Ip)	0.9	0.099
Sdhc	AI009817	Succinate dehydrogenase complex, subunit C, integral membrane protein	0.7	0.001*
Sdhd	AI410703	Succinate dehydrogenase complex, subunit D, integral membrane protein	1.0	0.911
Sdhd	AI176608	Succinate dehydrogenase complex, subunit D, integral membrane protein	0.8	0.009*
Sucla2	BF412750	Succinate-CoA ligase, ADP-forming, beta subunit	0.9	0.680
Sucla2	H31112	Succinate-CoA ligase, ADP-forming, beta subunit	0.6	0.596
Sucla2	AA923982	Succinate-CoA ligase, ADP-forming, beta subunit	0.7	0.001*
Suclg1	NM_053752	Succinate-CoA ligase, alpha subunit	0.5	0.000*
Suclg2	AI237518	Succinate-CoA ligase, GDP-forming, beta subunit	0.4	0.000*
Tpi1	NM_022922	Triosephosphate isomerase 1	3.0	0.001*
Uox	M24396	Urate oxidase	0.1	0.221[a]

Table IV. *Continued*

Gene symbol	Representative public ID	Gene title	Fold	*P*-value
Upb1	NM_053845	Ureidopropionase, beta	0.1	0.387[a]
Upp1	BI292558	Uridine phosphorylase 1	9.8	0.000*
Xdh	NM_017154	Xanthine dehydrogenase	2.5	0.001*

Expression levels of mRNAs related to glycolysis, the TCA cycle, fatty acid synthesis, nucleotide metabolism and the arachidonic acid cascade are shown. Pancreatic tissues derived from PDAC rats ($n = 6$) and controls ($n = 4$) were analyzed. *P*-values were calculated using Student's *t*-test.
[a]Expression levels were too low to be analyzed accurately by microarray analysis.
*$P < 0.05$.

Discussion

Serum metabolites are ideal biomarkers of human disease as the collection of serum samples is relatively non-invasive and multiple samples can be obtained to monitor disease progression. However, since serum represents the effects of metabolism in multiple organs, it is difficult to assign a metabolic fingerprint to specific metabolic processes of disease. Despite this, metabolites that change in the serum and display a similar change in diseased tissue, such as a cancerous lesion, are potential biomarkers specific to the metabolic process of the disease.

In this study, sera and pancreatic tissues from four control and six PDAC rats were subjected to non-targeted and targeted GC-MS-based metabolomics. The PCA score plots of the non-targeted metabolomic data of both the serum and pancreatic tissue showed a clear separation between control and PDAC rats, indicating the presence of distinct metabolite profiles in the serum and pancreatic tissue of PDAC-bearing rats compared with control rats.

Palmitoleic acid, which contributed to the distinctive metabolic profiles of the samples from the PDAC-bearing and control rats, was significantly decreased in the serum. Palmitoleic acid is a monounsaturated fatty acid biosynthesized from palmitic acid. Since palmitoleic acid is also contained in the diet, the decreases in the serum and pancreatic tissue of PDAC-bearing rats could be due to decreased absorption from the intestine. However, the decrease in PDAC-bearing rat lesions was apparently more pronounced in pancreatic tissue than in the serum. If the decrease in palmitoleic acid in the pancreatic tissue was due to its decreased levels in the serum, then the decreases found in the serum and pancreatic tissue should be similar. Instead, palmitoleic acid was decreased by a factor of ~2 in the serum and by a factor of ~7 or more in pancreatic tissue: while the decrease in palmitoleic acid in the pancreatic tissue of PDAC-bearing animals was not statistically different from the controls, it is notable that the highest level of palmitoleic acid in the PDAC rats was 13.77 p.p.m., whereas the lowest level of palmitoleic acid in the control rats was 100.33 p.p.m., a 7-fold difference. This suggests that decreased palmitoleic acid in pancreatic tissue was most likely due to increased consumption of the fatty acid in the PDAC lesions and that the decrease of palmitoleic acid in the serum was likely caused by its decrease in pancreatic tissues. Therefore, palmitoleic acid in the serum is a candidate biomarker for PDAC diagnosis.

In addition to palmitoleic acid, two other metabolites showed decreases in both the serum and pancreatic tissue: Arachidonic acid and 2(1*H*)-pyrimidinone were decreased non-significantly in the serum and decreased significantly in pancreatic tissue samples. Interestingly, the decrease of arachidonic acid could have been mediated by the increased expression of Alox5ap in PDAC (see Figure 3B). Increased activation of Alox5 could be the cause of the decrease of linoleic acid and arachidonic acid in the pancreatic tissue of PDAC-bearing rats. However, further investigations are needed to ascertain whether decreased linoleic acid and arachidonic acid were due to aberrant arachidonic acid metabolism or decreased synthesis of fatty acids.

One of the hallmarks of cancer is an increase of *de novo* fatty acid synthesis (16). A wide variety of tumors and their precursor lesions undergo exacerbated *de novo* biosynthesis of fatty acids from citrate by lipogenic enzymes—Acly, acetyl-CoA carboxylase and Fasn—irrespective of the levels of circulating lipids (16). In our study, however, we detected a decrease in the levels of several fatty acids. Possibly, decreased Acly expression (see Figure 3A) may have caused the decreases seen in the fatty acids in the pancreatic tissue of PDAC-bearing rats.

Another hallmark of cancer is the 'Warburg effect' (14,15) and decreased glucose has been reported in the serum and cancerous tissues of oral, colon and stomach cancer patients (17,18) and increased lactate has been reported in the serum of pancreatic cancer patients (19). In the present study, transcriptional analysis of PDAC tissues also suggested activation of anaerobic glycolysis and suppression of the TCA cycle. However, neither decreased glucose nor increased lactate were observed in the serum or pancreatic tissue of PDAC-bearing rats. The lack of a 'Warburg effect' in PDAC-bearing rats was probably due to the fact that after ~2 weeks of development, the PDACs were not advanced enough to disrupt pancreatic function and glucose control.

A notable difference between palmitoleic acid and glucose and lactic acid is that there are metabolic pathways dedicated to the regulation of glucose and lactic acid levels, but not to palmitoleic acid levels. Consequently, the tumor-mediated fluctuations in glucose and lactic acid seen in patients with more advanced tumors (17–19) may be absent in patients (and animal models) with less advanced tumors. In contrast, fluctuations of unregulated metabolites, such as palmitoleic acid, may occur in patients (and animal models) with less advanced tumors, as seen in the present study.

The increase in nucleotide degradation products xanthine, uridine and beta-alanine coupled with increased expression of several enzymes involved in nucleotide degradation (see Figure 3C) suggests that accelerated nucleotide degradation is occurring in the PDAC lesions. This accelerated nucleotide degradation may be due to the increased turnover of nucleotides in the PDAC lesions, which results from the increased nucleic acid synthesis in proliferating cells in the lesions.

Chenodeoxycholic acid, a major constituent of bile acids, was increased in the serum of PDAC-bearing rats. Metabolomic profiling of plasma of pancreas cancer patients by Urayama *et al.* (20) also showed an elevation of the bile acids taurocholic acid and tauroursodeoxycholic acid.

Concluding remarks

In summary, metabolites in the serum and pancreatic tissue of control and PDAC-bearing K-*ras*^{G12V} transgenic rats were analyzed by non-targeted and targeted GC-MS and transcripts in the PDAC lesions were analyzed by microarray. GC-MS analysis indicated that the profiles of the metabolites in the serum and pancreatic tissue samples derived from control rats differed from those derived from PDAC-bearing rats. A metabolite identified as palmitoleic acid was significantly decreased in the serum of PDAC-bearing rats and this decrease was likely due to its decrease in pancreatic tissue. Two other interesting metabolites are linoleic acid and arachidonic acid. These metabolites were significantly decreased in the pancreases of PDAC-bearing rats, possibly due to Alox5ap-mediated upregulation of Aox5 activity. Whether these metabolites could be markers of more advanced pancreas cancer remains to be determined. Finally, integration of the results of the non-targeted GC-MS analysis and transcriptomic

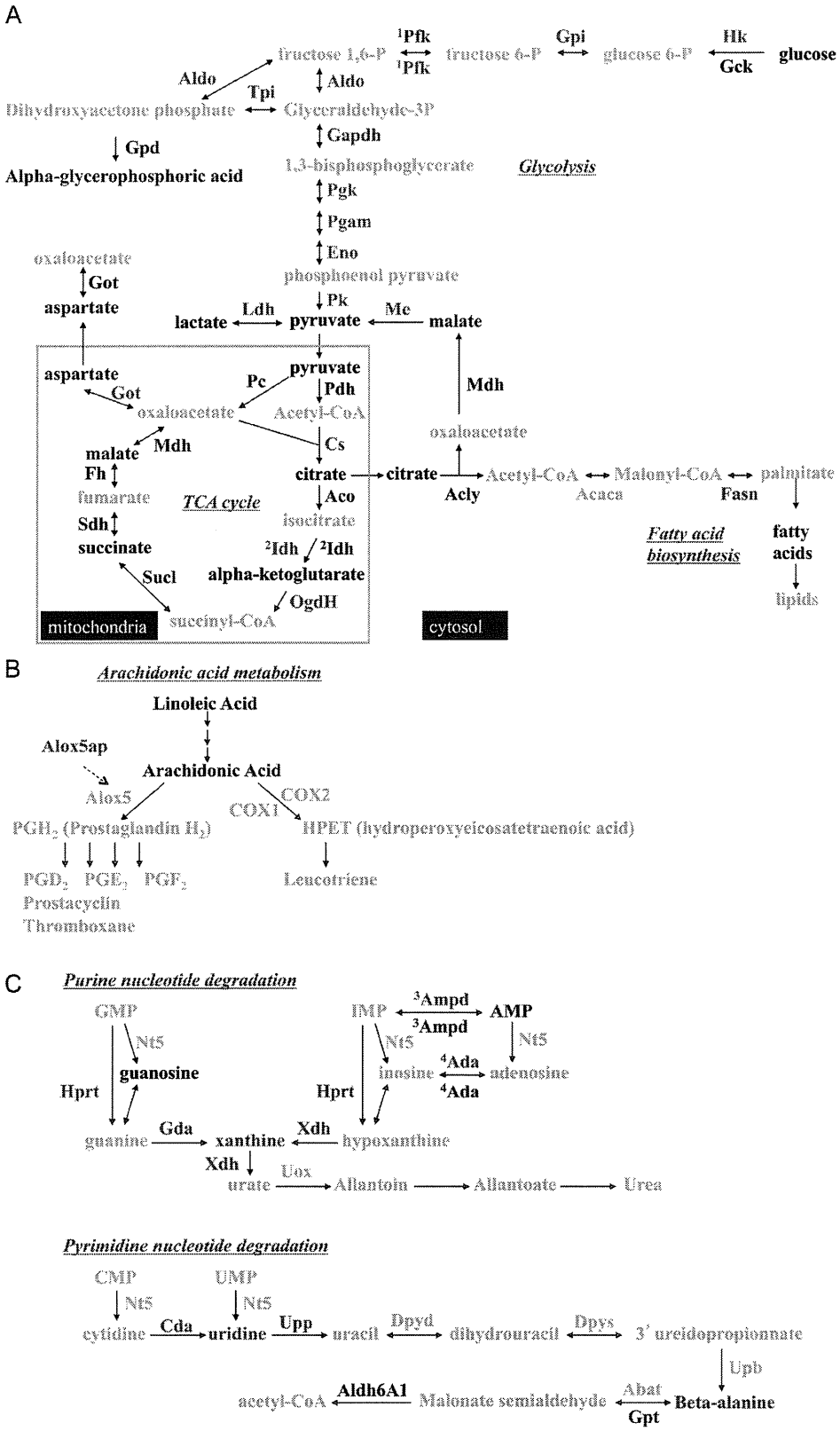

Fig. 3. Schematic representations of the most relevant metabolic and transcriptional differences in pancreatic tissues between PDAC and normal rats. Red, higher concentration in PDAC rats. Blue, lower concentration in PDAC rats. Black, not changed. Gray, not determined or unclear. [1]Pfkp was increased, whereas Pfkm was decreased. [2]Idh3a was increased, whereas Idh2, Idh3B and Idh3g were decreased. [3]Ampd3 was increased, whereas Ampd2 was decreased. [4]Ada, Adarb1 and Adarb2 were increased, whereas Adar was decreased.

analysis indicated accelerated anaerobic glycolysis and nucleotide degradation and suppressed TCA cycle and fatty acid biosynthesis in the PDAC lesions.

Supplementary material

Supplementary Table 1 and Figure 1 can be found at http://carcin.oxfordjournals.org/

Funding

Grant-in-Aid for Scientific Research (C) (19590401, 23590469) from Japan Society for the Promotion of Science. Grant-in-Aid for Cancer Research (15-2, 16-13, 17S-6, 20S-8) from the Ministry of Health, Labor and Welfare, Japan. Research on New Drug Development (H21-seibutsushigen-ippan-003) from the Ministry of Health, Labour, and Welfare, Japan. Research on Nanotechnical Medical (H19-nano-ippan-014) from the Ministry of Health, Labour, and Welfare, Japan. Health and Labour Sciences Research Grants (Research on Risk of Chemical Substance 21340601, H19-kagaku-ippan-006 and H22-kagaku-ippan-005, and H22-kagaku-ippan-005) from the Ministry of Health, Labour and Welfare, Japan.

Conflicts of Interest Statement: None declared.

References

1. Jemal,A. *et al.* (2003) Cancer statistics, 2003. *CA Cancer J. Clin.*, **53**, 5–26.
2. Akdogan,M. *et al.* (2001) Extraordinarily elevated CA19-9 in benign conditions: a case report and review of the literature. *Tumori*, **87**, 337–339.
3. Ni,X.G. *et al.* (2005) The clinical value of serum CEA, CA19-9, and CA242 in the diagnosis and prognosis of pancreatic cancer. *Eur. J. Surg. Oncol.*, **31**, 164–169.
4. Duffy,M.J. (1998) CA 19-9 as a marker for gastrointestinal cancers: a review. *Ann. Clin. Biochem.*, **35** (Pt 3), 364–370.
5. Ueda,S. *et al.* (2006) Ductal origin of pancreatic adenocarcinomas induced by conditional activation of a human Ha-ras oncogene in rat pancreas. *Carcinogenesis*, **27**, 2497–2510.
6. Fiehn,O. (2002) Metabolomics—the link between genotypes and phenotypes. *Plant Mol. Biol.*, **48**, 155–171.
7. Nicholson,J.K. *et al.* (1999) 'Metabonomics': understanding the metabolic responses of living systems to pathophysiological stimuli via multivariate statistical analysis of biological NMR spectroscopic data. *Xenobiotica*, **29**, 1181–1189.
8. Beckonert,O. *et al.* (2007) Metabolic profiling, metabolomic and metabonomic procedures for NMR spectroscopy of urine, plasma, serum and tissue extracts. *Nat. Protoc.*, **2**, 2692–2703.
9. Dettmer,K. *et al.* (2007) Mass spectrometry-based metabolomics. *Mass Spectrom. Rev.*, **26**, 51–78.
10. Weckwerth,W. *et al.* (2005) Metabolomics: from pattern recognition to biological interpretation. *Drug Discov. Today*, **10**, 1551–1558.
11. Sreekumar,A. *et al.* (2009) Metabolomic profiles delineate potential role for sarcosine in prostate cancer progression. *Nature*, **457**, 910–914.
12. Tanaka,H. *et al.* (2010) Mature acinar cells are refractory to carcinoma development by targeted activation of Ras oncogene in adult rats. *Cancer Sci.*, **101**, 341–346.
13. Fukamachi,K. *et al.* (2009) An animal model of preclinical diagnosis of pancreatic ductal adenocarcinomas. *Biochem. Biophys. Res. Commun.*, **390**, 636–641.
14. Garber,K. (2004) Energy boost: the Warburg effect returns in a new theory of cancer. *J. Natl Cancer Inst.*, **96**, 1805–1806.
15. Warburg,O. (1956) On the origin of cancer cells. *Science*, **123**, 309–314.
16. Menendez,J.A. *et al.* (2007) Fatty acid synthase and the lipogenic phenotype in cancer pathogenesis. *Nat. Rev. Cancer*, **7**, 763–777.
17. Tiziani,S. *et al.* (2009) Early stage diagnosis of oral cancer using 1H NMR-based metabolomics. *Neoplasia*, **11**, 269–276, 4p following 269.
18. Hirayama,A. *et al.* (2009) Quantitative metabolome profiling of colon and stomach cancer microenvironment by capillary electrophoresis time-of-flight mass spectrometry. *Cancer Res.*, **69**, 4918–4925.
19. Nishiumi,S. *et al.* (2010) Serum metabolomics as a novel diagnostic approach for pancreatic cancer. *Metabolomics*, **6**, 518–528.
20. Urayama,S. *et al.* (2010) Comprehensive mass spectrometry based metabolic profiling of blood plasma reveals potent discriminatory classifiers of pancreatic cancer. *Rapid Commun. Mass Spectrom.*, **24**, 613–620.

Received August 30, 2012; revised January 29, 2013; accepted February 3, 2013

Twenty-One Proteins Up-Regulated in Human H-*ras* Oncogene Transgenic Rat Pancreas Cancers are Up-Regulated in Human Pancreas Cancer

Setsuko Yabushita, MS,† Katsumi Fukamachi, PhD,‡ Fumitake Kikuchi, MS,*† Masakazu Ozaki, DVM, PhD,* Kaori Miyata, DVM, PhD,* Tokuo Sukata, PhD,* Yoshihito Deguchi, DVM,* Hajime Tanaka, MD, PhD,§ Anna Kakehashi, PhD,† Satoshi Kawamura, PhD,* Satoshi Uwagawa, PhD,* Hideki Wanibuchi, MD, PhD,† Masumi Suzui, MD, PhD,‡ David B. Alexander, PhD,‡|| and Hiroyuki Tsuda, MD, PhD||*

Objectives: We have established rat models of pancreatic ductal adenocarcinoma (PDAC) in which expression of a human H-*ras*^{G12V} or K-*ras*^{G12V} oncogene regulated by the *Cre/lox* system drives pancreatic carcinogenesis. Pancreatic ductal adenocarcinoma which develops in H-*ras*^{G12V} and K-*ras*^{G12V} transgenic rats is cytogenetically and histopathologically similar to human PDAC. The present study was designed to determine the feasibility of using the commercially available H-*ras*^{G12V} transgenic rat to find diagnostic protein biomarkers for human pancreatic cancer.

Methods: For an animal model to be useful for searching for protein biomarkers for a disease, it is essential that proteins that are up-regulated in the model are also up-regulated in humans. We used liquid chromatography-tandem mass spectrometry (LC-MS/MS) to compare H-*ras*^{G12V} transgenic rat PDAC with surrounding normal pancreas tissue.

Results: We identified 30 up-regulated proteins in the H-*ras*^{G12V} transgenic rat PDAC lesions; importantly, 21 human homologs of these 30 rat proteins are up-regulated in human pancreatic cancer patients.

Conclusions: These results indicate that numerous proteins that are up-regulated in H—*ras*^{G12V} transgenic rat PDAC are also up-regulated in human pancreatic cancer; therefore, this rat model can be used to search for diagnostic biomarkers for this disease.

Key Words: pancreatic cancer, transgenic rat model

(*Pancreas* 2013;42: 1034–1039)

Pancreatic cancer is diagnosed in approximately 1 person per 10,000 annually in the United States and is the fifth leading cause of cancer death. Most patients die within 1 year of diagnosis, and the 5-year survival rate is less than 5%.[1] Pancreatic ductal adenocarcinomas (PDACs) are diagnosed in 95% or more of the patients with pancreatic cancer. The most widely used marker for pancreatic cancer, CA19-9, is unfortunately also elevated in cases of benign cholangitis, pancreatitis, and other cancers[2–4]; and most importantly, CA-19-9 does not detect pancreatic cancer in its early stages of development.[5] Consequently, there is presently no valid approach for early detection of pancreatic cancer; and therefore, there is an urgent need for new and more specific and sensitive biomarkers for this disease.

Recently, a number of proteomic analyses of human PDAC lesions have been conducted in the search for candidate biomarkers.[6–17] The major limitation of these studies is that they are performed with patients with late-stage cancers. In addition, comparisons of patients with early-stage pancreatic cancer and patients with other diseases of the pancreas is needed. These limitations severely restrict the practical application of human studies to the early detection of pancreatic cancer.

Genetically engineered animal models allow for defined stages of tumor development, homogenized breeding, control of environmental conditions, and standardized blood sampling, thereby reducing biological and nonbiological heterogeneity. Therefore, discovery of biomarkers using suitable animal models for human PDAC is a practical alternative to using human samples. During the past decade, several genetically engineered mouse models of human PDAC have been developed.[18] The most promising models are based on mice with an endogenous, conditionally expressed *Kras*^{G12D} allele.[18–20] A low-resolution proteomic analysis of the serum of *LSL-KRAS*^{G12D} mice demonstrated the feasibility of using this animal model to search for serum biomarkers of PDAC,[20] and more recently, proteomic analyses of the serum of *KRas*^{G12D}*/Ink4a-Arf* mice have been reported.[21,22]

We have been focusing on developing a rat model of human pancreatic cancer.[23–25] One advantage of using rats is that their relatively large body and organ size facilitates surgical procedures; however, the more important aspect is that development of a rat model of human PDAC makes a new animal model system available to pancreatic cancer researchers. In our rat model, expression of oncogenic human H-*ras*^{G12V}[23,25] or K-*ras*^{G12V}[23,24] is regulated by the *Cre/lox* system. Targeted activation of H-*ras*^{G12V} or K-*ras*^{G12V} is accomplished by injection of a *Cre*-carrying adenovirus into the pancreatic ducts and acini through the common bile duct. H-*ras* and K-*ras* transgenic rats (H-*ras*^{G12V} and K-*ras*^{G12V} Tg rats) develop identical PDACs: Several weeks after injection, proliferative lesions in the duct epithelium, intercalated ducts, and centroacinar cells, but not acinar cells, become widespread. The histopathologic features of the early pancreatic intraepithelial neoplasia

From the *Environmental Health Science Laboratory, Sumitomo Chemical Co., Ltd., Osaka, Japan; †Department of Pathology, Osaka City University Graduate School of Medicine, Osaka, Japan; ‡Department of Molecular Toxicology, and §Department of Gastroenterology and Metabolism, Nagoya City University Graduate School of Medical Sciences, Nagoya, Japan; and ||Nanotoxicology Project, Nagoya City University, Nagoya, Japan.

Received for publication August 29, 2012; accepted December 21, 2012.

Reprints: Setsuko Yabushita, MS, Environmental Health Science Laboratory, Sumitomo Chemical Co, Ltd, 1-98, 3-chome, Kasugade-naka, Konohana-ku, Osaka 554-8558, Japan (e-mail: yabushitas@sc.sumitomo-chem.co.jp).

This study was supported by a Grant-in-Aid for Scientific Research (C) from Japan Society for the Promotion of Science.

The authors declare no conflict of interest.